MASTER'S THESIS MASTER ENERGY SCIENCE – UTRECHT UNIVERSITY

Understanding the evolution of electricity networks

Modeling a century of Dutch and Hungarian transmission grid growth

Rens Baardman BSc

March 5, 2023

SUPERVISOR
Prof. dr. Madeleine Gibescu, Utrecht University

SECOND READER
Dr. Elena M. Fumagalli, Utrecht University

HOST ORGANIZATION
Grid Integration Systems and Mobility group,
SLAC National Accelerator Laboratory

HOST SUPERVISOR
David P. Chassin, PhD

WORD COUNT
12017 words (main text without tables, graphs, and footnotes)

Abstract

Transmission grids can be modeled as networks, with the substations and plants as the nodes, and transmission lines as the edges. The present state of such a network is the result of a complex process of network growth and development, often spanning more than a century in time. Due to a lack of data on the historical state of transmission grids, it has been difficult to study this process.

In this thesis, we present a unique new dataset of the historical development of the Dutch transmission grid, reconstructed from hundreds of old maps. Using network analysis, we analyze the network evolution of Dutch grid and compare it an existing dataset of the Hungarian grid. After rapid early network growth, the networks mature in the 1970s, after which many important network characteristics stabilize. We also find that both networks exhibit strong preferential attachment, meaning that nodes with higher degrees are more likely to receive new connections. This leads to an exponential degree distribution.

We use a synthetic network generator to try to model the observed growth. Even though the model used is simple, the simulated networks comes close to the real-world evolution on a number of network characteristics. However, since there is no preferential attachment assumed, the degree distribution is concentrated at the lower degrees.

We also track the evolution of the network vulnerability, looking both at the topological vulnerability and the change in the optimal power flow after node removal. We find that the topological vulnerability of the real-world networks also stabilizes after the 1970s, although the Dutch networks vulnerability is higher than that of the Hungarian network. The synthetic networks however do not show a drop in vulnerability, and vulnerability stays much higher than those found in the real-world networks. We find little correlation between the topological vulnerability, and the vulnerability calculated using the optimal power flow.

Acknowledgments

During my research, I was hosted by the GISMo group at the SLAC National Accelerator Laboratory. I want to thank dr. David Chassin for the invitation and the warm welcome, and for the fun and fruitful discussions we have had during my stay. I would also like to thank all the other members of the GISMo group for the useful comments and questions they had on my research ideas. I am very grateful for having had this opportunity.

I would also like to thank my supervisor prof. dr. Madeleine Gibescu for making this transatlantic collaboration possible, for the overall guidance during the project, and for being willing to meet at rather unorthodox hours of the day to bridge the time zones.

For supplying the data on the historical Hungarian transmission grid and sharing his perspective on this research area, I am indebted to dr. Bálint Hartmann. I now know how much time goes into creating such a unique dataset, and how generous it is to share it.

The volunteers behind the HoogspanningsNet website and forum have created a one-of-a-kind resource on the intricacies of the Dutch transmission grid and its history. My research would not have been possible without the excellent Netkaart and the collection of historical maps published on their website. Specifically, I would like to thank Gerard Nachbar for locating the sources of the historical maps, and Hans Nienhuis for supplying a copy of the Netkaart data.

My stay in the United States has been made possible with the financial support of the foundations Bekker-la Bastide-Fonds, de Korinthiërs, Schuurman Schimmel–van Outeren, de Fundatie van de Vrijvrouwe van Renswoude te 's-Gravenhage, K.F. Hein Fonds, and de Fundatie van de Vrijvrouwe van Renswoude te Delft.

Contents

Chapter 1

Introduction

Electricity grids can be modeled as networks. In such a network, the nodes are electricity producers and substations. The links are the power lines connecting them. This is an abstraction of a real grid into a mathematical object, which allows for analysis using mathematical network theory. For example, an important criterion to ensure the reliability of a grid is the $N-1$ criterion. This means that if one node or one link is removed from a network, the network should have enough capacity left to meet the demand. This ensures redundancy, so that when a power plant, a substation, or a power line fails unexpectedly, the power supply is not interrupted because the electricity can be rerouted via a different connection. The $N-1$ criterion has become an important network criterion for the planning of future networks, and is a good example of the use of modeling electricity grids as networks.

The structure of the network thus determines some essential characteristics of the function of the grid. Understanding the properties of this structure is therefore paramount to explaining the current performance, and predicting future performance. Underlying the structure of a network is the process that created this network. The current network is the result of a long formative process, shaped continuously changing changing demands, costs, technologies, modes of ownership, political structures, and legal structures. If we can understand some of these underlying processes and principles, we might be able to better understand why the current network looks the way it does, where its strengths and weaknesses lie, and what the future might be holding.

One such simple model is the *preferential attachment model*. It proposes that many networks found in nature and society form in a step-by-step process. In this process, new nodes appear, which attach to existing nodes by some random process. This random process favors existing nodes which have more existing connections: well-connected nodes are *preferred*. This process leads to networks with an interesting distribution of the number of connections per node: there is a heavy tail, with a small number of highly connected nodes occupying a central place in the network. These networks are called *scale-free*.

The first studies analyzing the network structures of power grids suggested that power grids are also scale-free, hinting that a preferential attachment method might also be underlying the network growth of electricity grids. Later reports found different distributions of nodes connections in power grids, concluding that preferential attachment cannot be the sole mechanism by which power grids grow. The question to come up with other, better models is still open. An important demand of power grids is that they are reliable and resilient. They should have minimal outages and be able to recover from these outages quickly. This means the network structure needs to adapt over time to prevent vulnerabilities, while the load and quality demands increase. Good synthetic network models should be able to model this characteristic too.

In this thesis, we explore the connection between the processes shaping grid growth, and the resulting characteristics of power grids, by building a dataset of the historical Dutch transmission grid in which the network structure from 1931 to now is represented. We focus on transmission grids both because there is much more historical data available than for distribution grids, and because the meshed network structure is more interesting than radial networks. We can then study the change in network characteristics over time, and test synthetic model assumption about grid growth. We also analyze the vulnerability of the network in each year, and assess if the network is becoming more robust and whether the grid development manages to strengthen vulnerable points in the network.

1.1 Prior research

Multiple models have been proposed for the growth of electricity grids, which are used to generate synthetic electricity networks for the purpose of testing and analysis (see Section 2.4). However, we could only find two analyses of historical development of electricity networks: Buzna et al. (2009) studied the growth rate, 'topological efficiency' and vulnerability of the 400 kV layer of the French transmission network from 1960 to 2000, and Hartmann and Sugár (2021) studied the *small-world* and scale-free properties of the full Hungarian transmission network from 1949 to 2019. When a network is small-world, it means that the average shortest path length between two nodes is low, while the network is still highly clustered (Watts & Strogatz, 1998). This is an indication that nodes in the network are 'close' to each other, which leads to high information transfer speeds and improved synchronizability – important characteristics for a power grid. Hartmann and Sugár concluded that the Hungarian network is *not* scale-free, and that most network properties stabilized after the initial growth phase of around 20 years. They also compared the Hungarian network with a synthetic network simulated by Mei et al. (2011), concluding that they show remarkable similarities. But until now, there has been no validation of synthetic network models on the full evolution of real electricity networks, nor have the assumptions underlying these models been tested.

On the topic of changing vulnerability of power grids, Buzna et al. (2009) and Hartmann (2021) use the topological measure of *network efficiency* to determine how reliable power grids are. Vulnerability is then defined as the the drop in efficiency after one or more nodes or edges are removed: the lower the drop in efficiency, the less vulnerable a network is. Buzna et al. (2009) observe a rapidly decreasing vulnerability of the French transmission grid over time, with a decrease in critical nodes. This process continues over the entire analyzed time span from 1960 to 2000. Hartmann (2021) conclude that the Hungarian transmission network increased its tolerance to removals in the first decades of its growth, but that the vulnerability has remained relatively stable since the early 1980s. Using topological measures is a simple way to analyze network vulnerability, but they are a general network analysis tool that do not take into account the nature of power grids and its electrical properties. For example, the efficiency measure assumes that the path that electricity follows is the shortest path in the network sense, using the least amount of edges. But in reality, electrical parameters such as capacity and impedance of lines determine the flow of electricity. Topological measures are also not able to account for cascades, where the outage of one substation or line triggers the outage of different components. Such a domino-effect can only be modeled when power flows are taken into account.

1.2 Research question

The main literature gap is the lack of validation of existing synthetic network generating models on empirical data, and the fact that existing models do not take into account how grid development responds to failures. To close this gap, we use data on the historical development of the Dutch and Hungarian networks, and match the observed developments to the predictions from the synthetic network generators. The main research question is: **Which synthetic network generator can model the historical developments of the Dutch (1924–2021) and Hungarian (1949–2019) electric transmission networks?** We divide this question into the following sub-questions and research approach:

(A) **How did the Dutch and Hungarian transmission networks evolve over time?**

For the Hungarian grid, we use the data from Hartmann and Sugár (2021). For the Dutch grid we use historical maps. From these maps, we construct a digital version of the network. This is not a straightforward task, as there are many choices to be made during the digitization process. One of the questions is how large the influence of these choices is on the resulting network, and how sensitive the research conclusions are to this influence.

After that, we calculate important network characteristics for both networks throughout time. These characteristics include the degree distribution, small-worldness. This will also allow to answer the question at what point in time (if at all) the networks became scale-free, or whether a different degree distribution than a power-law is a better fit. This is important information for assessing the model performance later on.

(B) **Which existing synthetic network models fit the Dutch and Hungarian developments?**

There are many existing synthetic network models, with different purposes and underlying assump-

tions (see Section 2.4). The question is whether these assumptions hold in the Dutch and Hungarian cases, and to what extent the generated networks match the observed networks.

(C) **How did the vulnerability of the networks change over time?** When networks are growing, there is an opportunity to construct new components in such a way that they contribute to reliability, but the networks total load also increases so the potential for larger events does too. We use topological and power flow metrics to measure the evolution of the vulnerability over time, and try to relate this to changes in the networks structure. We also compare this to evolution of vulnerability in the synthetic network models.

1.3 Expected results

We have the following expected results, split out per sub-question:

(A) **On constructing the historical development:** Reconstructing the Dutch and Hungarian grids will shine a light on different phases of network development. We expect to see different growth behaviors depending on the network size: a small, beginning network grows in a different way than a larger, mature network. It might also show different market regimes, with a transition from state-owned to liberalized electricity markets around 2004 (for both the Netherlands and Hungary). Different regulation regimes with different quality and reliability standards can also influence the network structure. Ajodhia et al. (2006) for example compare different regulation instruments between countries, concluding that "especially in Italy, network quality improved significantly, after the incentive schemes were introduced".

For the Hungarian network, the calculated network characteristics should reproduce the results from Hartmann and Sugár (2021). Based on the literature, we expect that the best fit to the degree distribution for the Dutch network is an exponential distribution (see Section 2.2.2). This means that the Dutch network is *not* scale-free. How the network is constructed can have an influence on the degree distribution. The Dutch network will probably show small-world characteristics after the initial stages, especially when there are multiple voltages levels.

(B) **On assessing existing models:** As Hartmann and Sugár (2021) note, the last year of the Hungarian network is well matched by the synthetic network generated by Mei et al. (2011). We expect that the Dutch network can also be well matched by the model from Mei et al. (2011) or a similar model. Models which can be tweaked to historical conditions, have a spatial and a temporal output, and can model multiple voltages will probably deliver the best results. Also, models which are designed with a mesh architecture in mind are probably the best fits for both countries, since transmission grids often have a mesh structure.

(C) **On determining changes in network vulnerability:** We expect that the network topology changes over time in such a way that network failures have a decreasing effect. This means the network becomes more reliable, although Hartmann (2021) notes that for the Hungarian network, the vulnerability stabilized already in the late 1970s, so something similar might occur in the Dutch grid. Strategies which we expect to find are creating ring structures (meshes), so there are redundant paths between nodes, and using higher voltage layers to connect lower voltage layers in a redundant way.

1.4 Relevance and applications

Finding answers to the research questions can lead to many relevant applications, both theoretical and practical:

(A) **On constructing the historical development:** The results will add to the ongoing debate on the structure and growth of electricity networks, specifically whether and how they become scale-free and small-world. For the Netherlands and Hungary, the results can add to the knowledge on the history of the power grids from a network perspective. My research will also show the effect of different choices in the process of abstracting an electricity grid into a network model, hopefully leading to a more standardized way of creating network models. To support further research on network growth, we will release the first open source dataset of the historical evolution of a power grid.

(B) **On assessing existing models:** Assessing the model fit of existing synthetic network models will be the first attempt to validate these models on an entire network evolution, based on historical data. It will also show which assumptions from the models are valid, and which need to be altered. This allows further development of more accurate models which can generate the whole evolution of a network, can model the age of components, and can model the geographical layout of a grid to also capture e.g. the line length and the number of graph crossings (see Birchfield and Overbye (2021)).

(C) **On determining changes in network vulnerability:** Understanding when and how the network vulnerability changed due to changes in the network structure, can allow us to understand how networks can be made more reliable. It can also point to current bottlenecks in the networks. Finally, we can improve synthetic network generators by observing the design strategies that are used to decrease networks vulnerability.

Chapter 2

Theoretical background

2.1 Network terminology

We define a *network* G as a set of *nodes* and *edges*: $G = (V, E)$ where V is the set of nodes (also called *vertices*), and E is the set of edges. The number of nodes is $n := |V|$, and the number of edges if $m := |E|$. An edge is denoted as a pair (i, j), where i and j are nodes in V. In our analysis, we only consider *undirected* networks, so the edge (i, j) is the same as the edge (j, i). We also do not take *self-loops* into account, edges from and to the same node, e.g. (i, i). We do consider parallel edges, so multiple distinct edges (i, j) are possible. Networks with parallel edges are called *multigraphs*. We can also collapse parallel edges into a single edge, so the network becomes a *simple graph*.

For a node $i \in V$, the *degree* k_i is the number of edges connecting i. Formally:

$$k_i := |\{(i, j) \in E \mid j \in V\}|$$

The average degree $\overline{k}$ is

$$\overline{k} := \frac{1}{n} \sum_{i \in V} k_i = \frac{2 \cdot m}{n}.$$

Here, the last expression follows from the observation that if you sum the degrees of all nodes, you count every edge twice. The *neighborhood* N_i of node i is the set of nodes with which it is connected:

$$N_i := \{j \in V \mid (i, j) \in E\}.$$

For simple graphs, we have $k_i = |N_i|$, but this is not true for nodes with parallel edges since then $k_i > |N_i|$. For some integer k, the *k-core* of a network is the largest subnetwork such that all nodes have degree at least k. It can be formed by iteratively removing nodes from the network with degree less than k.

A *path* between i and j is a sequence of edges, where the first edge starts in i, the last edge ends in j, and all intermediate edges connect to each other. The *length* of a path is the number of edges in the path. The *shortest path length* (or *distance*) between i and j is denoted with $d(i, j)$. The *average shortest path length* L is then:

$$L := \frac{1}{n(n-1)} \sum_{i,j \in V, i \neq j} d(i, j).$$

The *diameter* is the maximum distance between two nodes in the graph. This is the length of the longest shortest path.

The *local clustering coefficient* C_i of node i measures to what extent its neighbors are connected to each other. It considers all pairs of neighbors of i, and calculates the share of these neighbors that are connected to each other:

$$C_i := \frac{2 \cdot |\{(j, \ell) \in E \mid j, \ell \in N_i\}|}{|N_i| \cdot (|N_i| - 1)}.$$

The factor 2 comes from the fact that we are considering all pairs of neighbors, and each pair occurs twice but in reverse order. The *average clustering coefficient* $\overline{C}$ of a graph is then

$$\overline{C} := \frac{1}{n} \sum_{i \in V} C_i.$$

An example network and calculation of its network properties is given in Figure 2.1.

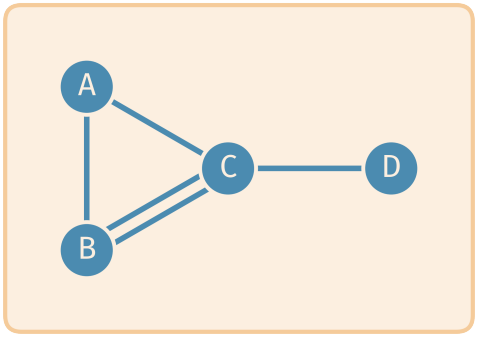

Figure 2.1: An example network consisting of four nodes ($n = 4$) and five edges ($m = 5$). There are two parallel edges between nodes B and C. Node A has two connected edges, so $k_{\mathsf{A}} = 2$. We see $k_{\mathsf{B}} = 3$, $k_{\mathsf{C}} = 4$, and $k_{\mathsf{D}} = 1$, so the average degree $\overline{k}$ is 2.5. The 2-core consists of the nodes A, B, and C and the edges between them. Node D is excluded because its degree is less than 2. The 3-core is the empty network: even though nodes B and C are initially of degree at least 3, they are of degree 2 after pruning nodes A and D, so they are also pruned.
The shortest path between nodes A and D is using edges (A, C) and (C, D), so $d(\mathsf{A}, \mathsf{D}) = 2$. Similarly $d(\mathsf{B}, \mathsf{D}) = 2$. All other distances are 1, so the average shortest path length L is $1\frac{1}{3}$. The diameter is 2.
The clustering coefficient of node A is 1, since its neighbors B and C are connected. For node C, we have $C_{\mathsf{C}} = \frac{1}{3}$ since nodes A and B are connected, but node D is not connected to either A or B. For nodes with degree 0 or 1, the clustering coefficient is not properly defined, but is often taken as 0. Following that convention, we get an average clustering coefficient $\overline{C}$ of $\frac{7}{12}$.

2.1.1 Weighted networks

If we assign a *weight* to all edges of a network we get a *weighted network*. The weight can have various meanings, but it is often related to the importance, strength, capacity, or cost of an edge. All previously mentioned network terms also have a weighted equivalent, taking into account the edge weights. Most relevant to our analysis are the *weighted length* of a path and the *weighted distance* between nodes. The weighted length of a path is the sum of the weight of the edges in the path. The weighted distance $d^w(i, j)$ between nodes i and j is the shortest weighted length of a path between the two nodes.

When we trivially set the weights of all edges to 1, these definitions agree with their unweighted counterparts, and we get back the *topological* length and distance as defined before. This is certainly not true in general, and choosing the right weights for a problem can unveil a different structure in a network. For electrical networks, we are interested in the general concept of distance between nodes. A simplest distance measure would be to use the *geometric* distance between two nodes. More advanced measures include various definitions of *electrical* distances. For example, we can set the weight of an edge to be the resistance of the transmission line between two nodes. Then the length of a path becomes the sum of resistances of the edges in the path, which is similar to how resistances can be summed when calculating the equivalent resistance of resistors in series.[1] Similarly, we can set as weights the magnitude of the impedance of a line, to also capture the reactance of a transmission line.

2.2 Degree distributions

The *degree distribution* of a network is the theoretical or observed probability of nodes having a certain degree. The degree distribution helps distinguish networks where nodes are likely to have a degree close to the average from networks with a larger spread of degrees. The first category contains regular structures such as rings and lattices, while networks in the second category can have nodes with a high degree that can function as hubs. Differences in degree distributions are a good sign that the underlying network structures are also different.

[1] Note that this method does not give the equivalent resistance between two nodes in general, since resistors in parallel paths are not taken into account. The more general distance metric *resistance distance* (Klein & Randić, 1993) does calculate the equivalent resistance between two nodes, but is not as simple as calculating the shortest weighted length between nodes.

2.2.1 Scale-free networks

A special class of networks are those with a degree distribution that follows a *power law*. This means that the probability that the degree k of a node is equal to an integer x is given by:

$$\mathbb{P}(k = x) \propto x^{-\gamma}.$$

Here, γ is the *exponent* of the distribution, and it usually lies between 2 and 3. Networks with such a degree distribution are called *scale-free networks*. Important properties of scale-free networks are that they have a heavy tail, so that there are a significant number of highly connected nodes, and that there is no characteristic 'scale' around which the degrees cluster (hence the term 'scale-free'). This is in contrast to networks with degree distributions that have a strong peak around the average degree, and no heavy tail.

Some researchers have found that certain power grids show such a scale-free structure, such as the electricity network in the Western U.S. ($\gamma \approx 4$, according to A.-L. Barabási and Albert (1999); $\gamma = 3.0$ according to Chassin and Posse (2005)), and also in the Eastern U.S. ($\gamma = 3.1$) (Chassin & Posse, 2005). This is remarkable, because there are networks from many different research areas which are also found to be scale-free. Examples include in-coming links to web pages ($\gamma = 2.1$) (Broder et al., 2000), friendships between users of the Dutch social network Hyves (γ between 2.0 and 3.0) (Clauset et al., 2009, Table I, HY), the connections between different internet subnetworks ($\gamma = 2.2$) (Faloutsos et al., 1999, Table 8), citations between scientific papers (for incoming citations: γ between 2.5 and 3) (Price, 1965), and metabolic interactions between yeast proteins (γ between 3.1 and 3.9) (Clauset et al., 2009, Table I, Mp). From a grid reliability viewpoint, it is also interesting that grids are scale-free, because certain scale-free networks are highly robust to removal of randomly chosen nodes (Albert et al., 2000).

Different methods have been developed to determine whether a network is scale-free. The simplest method is based on the fact that when you graph a power law on a log-log plot, it shows up as a straight line. Hence, given a network, you can construct the degree distribution and make a log-log plot of the degree vs. the frequency of nodes with that degree. If the data points follow a 'straight enough line', then you conclude that the degree distribution follows a power law, and hence that the network is scale-free. This line can also be fitted using linear regression, from which you can calculate an R-square value to determine the goodness of fit.

This method has received criticism, because it is relatively easy to 'see' straight lines on a log-log plot, even though a power law might not be the best fit. An alternative is to consider different distributions, and compare the goodness of fit with a suitable test. As an example, Holmgren (2006) used a Kolmogorov-Smirnov test and a chi-square test to conclude that an exponential distribution was not a good fit for their degree distribution. More recent developments include using maximum-likelihood methods to find the best fit for γ (Clauset et al., 2009), and likelihood-ratio tests to compare different distributions (Broido & Clauset, 2019).

2.2.2 Are power grids scale-free?

There is no general best fit to empirical degree distributions of power grids. One of the first fits by A.-L. Barabási and Albert (1999) was a power law, but since then only one other paper has fitted a power law to a degree distribution (Chassin & Posse, 2005). The most common fit so far seems to be an exponential degree distribution, as can be seen in Table 2.1. From this, it appears that power grids are probably *not* scale-free.

The lack of consensus can be explained by different factors. First of all, there seems to be no agreed upon approach yet to evaluate the goodness of fit of proposed models. More recent advances in statistical methods might be able to resolve this issue. A good overview of these new methods is given by Holme (2019). Another possible reason for the lack of a universal fit comes from the different natures of the grids studied. The U.S. grids studied are larger and have a higher maximum degree compared to grids of European countries, or even compared to the whole European grid. Since a power-law fit works best when there is a large spread of degrees, this could explain why the only power-law fits have been found for a U.S. grid. Finally, some authors distinguish between approximations for the lower degree nodes – which might show power-law behavior – and for the tail with higher degree nodes – which often has a sharper exponential cut-off.

Table 2.1: Overview of fits to empirical degree distributions of power grids, as found in the literature. The parameters refer to the formulas for the probability density functions of the distributions: $\mathbb{P}(k = x) \propto x^{-\gamma}$ for the power law, and $\mathbb{P}(k = x) = \lambda e^{-\lambda x}$ for the exponential distribution.

Region	Degree distribution	Parameters	Reference
China, Anhui province	exponential	$\lambda = 0.65$	Han and Ding (2011)
China, East	exponential	$\lambda = 0.58$	Han and Ding (2011)
Europe (UCTE and different countries)	exponential	$\lambda = 0.56$ (UCTE), 0.37 to 1.10 (countries)	Rosas-Casals et al. (2007)
Hungary	exponential (a.o.)	$\lambda = 0.67$ (2019)	Hartmann and Sugár (2021)
Italy	exponential	$\lambda = 0.55$	Crucitti et al. (2004)
Italy, France & Spain	mix of Gaussians		Rosato et al. (2007)
Netherlands, North (medium voltage)	mix of exponential with power-law tail		Pagani and Aiello (2011)
Nordic countries	exponential		Holmgren (2006)
North America	exponential	$\lambda = 0.5$	Albert et al. (2004)
Poland	exponential		Cloteaux (2013)
U.S., Eastern	power law	$\gamma = 3.1$	Chassin and Posse (2005)
U.S. Eastern, Western and Texas (ERCOT)	exponential		Cotilla-Sanchez et al. (2012)
U.S., NYISO	sum of exponential and irregular random variable		Wang et al. (2010)
U.S., Southern California	exponential		Amaral et al. (2000)
U.S., Western	power law	$\gamma \approx 4$	A.-L. Barabási and Albert (1999)
U.S., Western	power law	$\gamma = 3.0$	Chassin and Posse (2005)
U.S., Western	sum of exponential and irregular random variable		Wang et al. (2010)

2.2.3 Performing statistics on the PDF or CDF

A technical note: while it is possible to plot and use statistical methods on the PDF of a degree distribution, it is often easier to use the *cumulative distribution function* (CDF) or the *complementary cumulative distribution function* (CCDF). If the PDF is given by some function $f(x) := \mathbb{P}(k = x)$, then the CDF $F(x)$ is given by:

$$F(x) := \mathbb{P}(k \leq x) = \int_0^x f(t)\, dt.$$

The CCDF $\bar{F}(x)$ is defined as the complement of the CDF:

$$\bar{F}(x) := \mathbb{P}(k > x) = 1 - \mathbb{P}(k \leq x) = 1 - F(x).$$

The advantage of using the CDF or CCDF is that there are no gaps for degrees which don't occur in the network, which makes it easier to plot. Perhaps more importantly, the function is monotonically increasing (CDF) or decreasing (CCDF), which makes it easier to determine the behavior of the distribution, as can be seen in Figure 2.2.[2]

[2]It is important to note that the perceived parameter of a distribution can change when switching from the PDF to the CDF. For a power-law distribution, we have $f(x) \propto x^{-\gamma}$ but $F(x) \propto x^{-(\gamma-1)}$, so the scaling parameter on a plot for $F(x)$ is $\gamma - 1$.

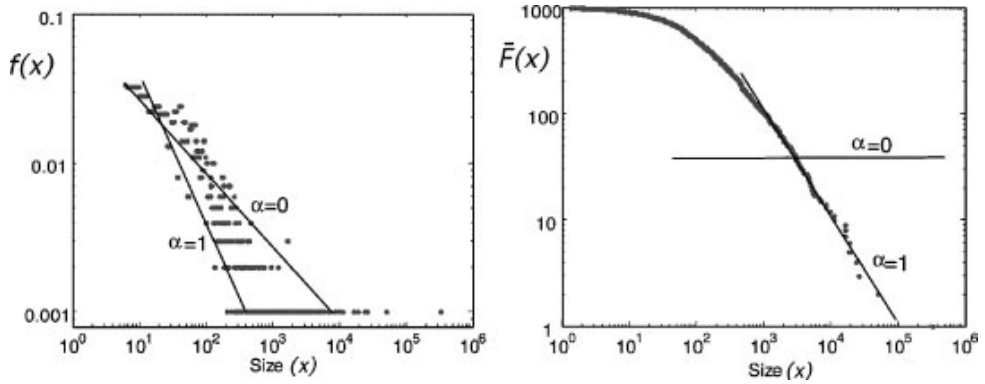

Figure 2.2: Samples from two power-law distributions, one with exponent $\gamma = \alpha + 1 = 1$, and one with $\gamma = 2$, plotted on log-log scale. The left graph shows the PDF and the right graph shows the CCDF. The effect of the different exponents on the behavior of the distribution can be seen much clearer in the right plot than in the left plot. From Fox Keller (2005, Figure 2).

2.3 Small-worldness

A network is consider *small-world* when it show strong local clustering, while also having a low average distance between nodes. This is in comparison to an *(Erdős-Rényi) random network* with the same number of nodes and edges. This random network model is perhaps the simplest model to generate random networks: given parameters n and m, it samples uniformly from all possible networks with n nodes and m edges (Erdős & Rényi, 1959). This means the likelihood that there is an edge between any given pair of nodes is $m/(n(n-1))$. Watts and Strogatz (1998) then propose to take a regular lattice-like structure with n nodes and m edges and randomly rewire every edge with a probability p. When $p = 0$ this gives the lattice structure, which has a high local clustering but a longer average distance. With $p = 1$ you get a random network with low average distance but little local clustering. They then observe that if you choose a p somewhere between 0 and 1, you can end up with a network that exhibits both high local clustering and a low average distance. They call these networks small-world, because due to the low distance every pair of node is just a couple of steps away from each other.

There are many examples of networks that exhibit small-world properties, from social, technical and economical areas (Amaral et al., 2000). Researcher have also found that power grids show small-world behavior, although one study of 15 European transmission systems concluded that this is only true when all voltage levels are considered together (Espejo et al., 2018).

There are multiple metrics available to determine whether a network is consider small-world. The easiest to calculate is the small-world coefficient σ:

$$\sigma := \frac{\overline{C}/C_r}{L/L_r}.$$

Here C_r and L_r are respectively the (global) clustering coefficient and the average distance of a random network of the same size as the network we consider. Then if $\sigma > 1$, we consider a network to be small-world.

2.4 Synthetic network models

There are various *synthetic network models*, which try to generate a network model which is comparable to power grids found in the real world. There are many differences between these models: both in types of networks they target (distribution vs. transmission, radial vs. ring based designs), assumptions they make about network development, and type of output (e.g. including geographic position of nodes or not). An overview of some of these models and their characteristics is given in Table 2.2.

2.4.1 Small-World Power Grid Growth and Evolution Model

The *Small-World Power Grid Growth and Evolution Model* from Mei et al. (2011, Section 4.3) is of particular interest for our research, due to the fact that its output is both temporal and spatial. The

Table 2.2: Overview of different synthetic model generators and their characteristics. 'Spatial' means whether the model output includes spatial information on the network. 'Temporal' means whether the algorithm builds the model in steps relating to the time evolution of the network. 'Voltages' is whether there are multiple voltage levels in the model. 'Tunable' means whether you can tune the degree distribution of the resulting model to match a certain arbitrary degree distribution. 'Result' is the default degree distribution of the resulting model.

Reference	Spatial	Temporal	Voltages	Tunable	Result
Birchfield et al. (2017)	yes	no	yes	yes	depends on input
Cloteaux (2013)	yes	no	no	yes	exponential
Deka et al. (2017)	yes	yes	no	partially	sum of shifted exponentials
Mei et al. (2011)	yes	yes	yes	no	unknown
Schweitzer et al. (2017)	no	no	no	yes	mixed model of Gamma distributions
Wang et al. (2010)	no	no	no	parameters	unknown

algorithm is based on a small number of assumptions which we can validate in the observed network growth. The simulation grows a transmission network on an $\ell \times \ell$-sized grid of points. The simulation time t has a resolution of one year. We assume there is an energy distribution function $P_S(x, y, t)$ that specifies the available power in MW at grid point (x, y) in year t. Similarly, the load demand distribution $P_D(x, y, t)$ specifies the demand in MW at a grid point. Both values can change over time for a specific grid point: for example when advancements in energy technologies make it possible to harness more power at a specific site, or when the load demand increases due to population growth.

The algorithm takes parameters a, b and p, and requires two other functions ϕ_S and ϕ_D. It proceeds as follows:

1. Every year, a new power plants are added to the network. The power plants are placed on the unoccupied grid points with the highest values for P_S. The capacity and voltage of a new plant is dependent on the available energy, and is given by applying ϕ_S on P_S.
2. Every year, b new substations are added to the network. The substations are placed on the unoccupied grid points with the highest values for P_D. The capacity and voltage of a new substation is dependent on the load demand, and is given by applying ϕ_D on P_D.
3. New power plants and substations are connected to the closest substation at their voltage level. If there is no substation at that voltage level, it will connect at the first possible lower voltage level. With probability p, a second connection is made to the second-closest substation.

As suggested parameters, Mei et al. (2011) use $\ell = 200$, $a = 1$, $b = 5$, and $p = 0.1$. The function P_S is defined in such a way that in the first 20 years all values are below 200 MW, the next 20 years the values are between 200 MW and 400 MW, and the last 10 years the values are above 400 MW. The values for P_D are sampled from a normal distribution with an average of 500 and a standard deviation of 150. The function ϕ_S samples capacities from a normal distribution. When the available power is below 500 MW, the voltage is set at 110 kV and the distributions average initially at 100 MW. Between 500 MW and 1000 MW it is set at 220 kV and 300 MW, and above 1000 MW at 500 KV and 600 MW. Furthermore, the average capacity of new power plants increases each year with $\alpha = 5\%$. The function ϕ_D works similar to ϕ_S, but the cutoffs are at 200 MW and 400 MW. The substations are sized larger than their demands, at 200 MW (demand below 200 MW), 500 MW (demand between 200 MW and 400 MW), and 1000 MW (demand above 400 MW). The annual increase in capacity is $\beta = 1\%$. The results of two example runs with these parameters are given in Figure 2.3.

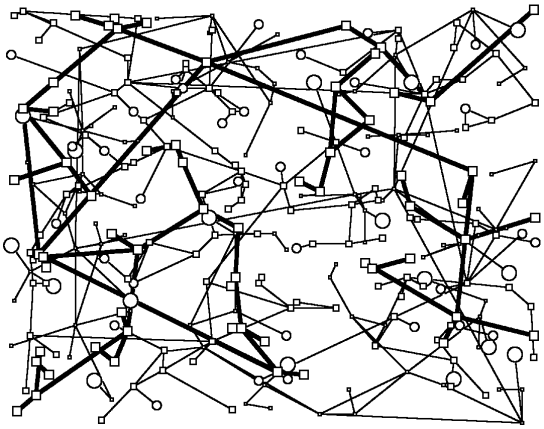

(a) "Snapshot at the 50th year of the power grid evolution" (Mei et al., 2011, Figure 4.6.e). The circles represent power plants and the squares are for substations. There are three voltage levels (110kV, 220 kV and 500 kV), visualized by increasing thickness of the lines.

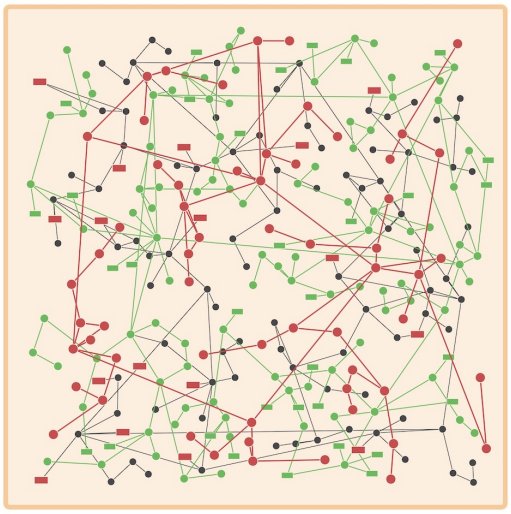

(b) Recreated simulation, using the same parameters.

Figure 2.3: Simulation results following the algorithm from Mei et al. (2011). The simulation is run for 50 years on a 200×200 grid. Each year $a = 1$ power plant and $b = 5$ substations are added. New nodes are connected to the closest substation, and with probability $p = 0.1$ also to the second-closest substation.

2.5 Vulnerability and reliability metrics

There are many ways to operationalize different ideas of vulnerability and reliability. Topological measures, which can be calculated using only the topological structure of a network, are the easiest to calculate. This brings they advantage that it is possible to compare these measures across different networks. However, the flow of electricity on electrical grids is not only dependent on the topology, but also on a number of electrical parameters. To understand the actual flow and the impact of events on the flow, we also consider metrics based on the power flow.

2.5.1 Topological metrics

A networks *efficiency* η is defined as the average inverse of the distance (Latora & Marchiori, 2001):

$$\eta(G) := \frac{1}{n(n-1)} \sum_{i,j \in V, i \neq j} \frac{1}{d(i,j)}.$$

This measure is based on the idea that transmission over a network (of information, electricity, or some other flow) is more efficient if the average distance between nodes is low. We can then calculate the drop in efficiency if a node is removed from the network, relative to the initial efficiency of the network. This is the called the *information centrality* of a node (Latora & Marchiori, 2007). For a node i, the information centrality $c_I(i)$ is given by:

$$c_I(i) := \frac{\eta(G) - \eta(G \setminus i)}{\eta(G)},$$

where $G \setminus i$ is the network with node i and its connected edges removed. If there are nodes with a high information centrality, this indicates that a network is vulnerable to the loss of these nodes. We can therefore calculate the maximum information centrality over the nodes, and use this is a measure of a networks vulnerability:

$$c_I(G) := \max_{i \in V} c_I(i).$$

We can also calculate the weighted version of a networks efficiency, where instead of using the topological distance $d(i,j)$, we use the weighted distance $d^w(i,j)$. In order to compare the weighted efficiency across networks of different sizes, Latora and Marchiori (2001) propose normalizing the weighted efficiency by comparing a networks efficiency to the best possible efficiency, where all nodes are connected to each

other. In the case where we use the topological distance, the optimal efficiency is 1, but this is not true in general if we use geometric distance between points in space, for example. So, we have:

$$\eta^w(G) := \frac{1}{n(n-1)} \left(\sum_{i,j \in V, i \neq j} \frac{1}{d^w(i,j)} \right) / \left(\sum_{i,j \in V, i \neq j} \frac{1}{d^w_{\text{opt}}(i,j)} \right),$$

where $d^w_{\text{opt}}(i,j)$ is the shortest possible distance between nodes i and j. Then the weighted vulnerability measure is:

$$c^w_I(G) := \max_{i \in V} \frac{\eta^w(G) - \eta^w(G \setminus i)}{\eta^w(G)}.$$

For electrical networks, it is interesting to note that if we use line resistance as our weighted distance, the weighted efficiency is the average *electrical conductance* of the shortest paths. If we use the approximation that specific resistances are the same for all lines in a network, using the length of the lines instead of the resistance leads to the same outcome.

2.5.2 Power flow metrics

We use the *loss of load* after the removal of a node, to measure the vulnerability of an electricity network to the removal of that node. To calculate the load loss, we first have to calculate the power flow on the entire network (see Section 3.3). Then, we remove a node, and still try to find a possible power flow by reducing the loads of other nodes ('load shedding'). Then, we use as loss of load the amount of load we had to reduce from other nodes, to still get a flow solution.

Chapter 3

Methodology

3.1 Reconstructing the historical Dutch and Hungarian grids

3.1.1 Data collection

We use historical maps to reconstruct the history of the Dutch transmission network. A sample of these maps is depicted in Figure 3.1.[1] Appendix B gives an overview of the maps and other sources used to reconstruct the historical Dutch grid.

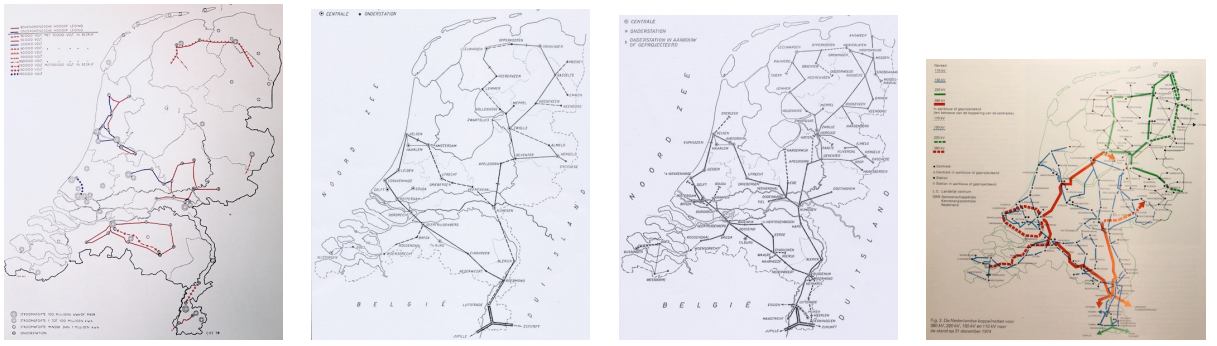

(a) 1938 **(b)** 1949 **(c)** 1960 **(d)** 1975

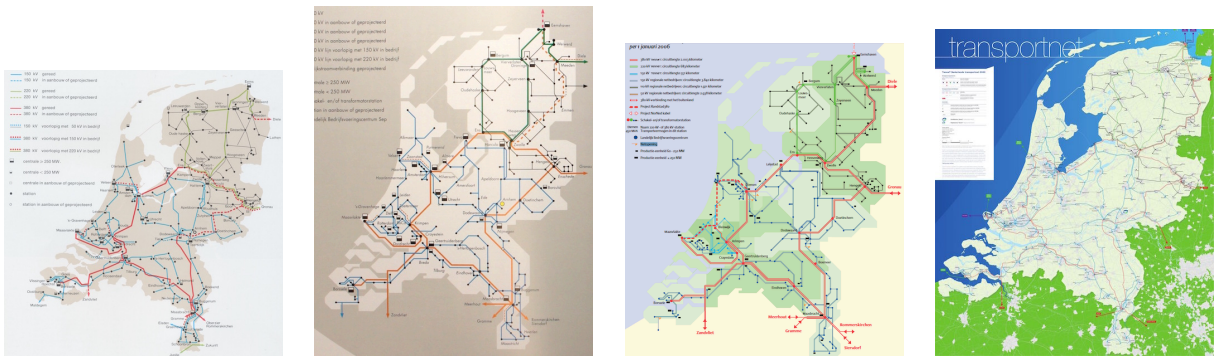

(e) 1984 **(f)** 1994 **(g)** 2006 **(h)** 2020

Figure 3.1: A sample of the historical maps of the Dutch grid. Sources in chronological order: CBS (1941a), SEP (1950), SEP (1961), SEP (1976), SEP (1985), SEP/EnergieNed (1995), TenneT (2006), TenneT (2020a).

[1] An excellent collections of historical maps is curated by the volunteers behind Hoogspanningsnet.com, which has been an invaluable source in finding historical references.

3.1.2 Constructing networks from power grids

Even though often little explanation is given about the process of creating a network model for a power grid, the choices made in this process can have a significant impact on the resulting network and its characteristics. An example of these types of choices is given in Figure 3.2, which gives three different methods to abstract a power grid into a network model. The version 'with tap' has three types of nodes: power plants, substations, and junctions.[2] This version has the highest number of nodes, and the most complex structure. On the other hand, the third version 'without taps reduced' only has power plants and substations as nodes, and has the simplest structure. The topologies of these options are different, leading also to different degree distributions.

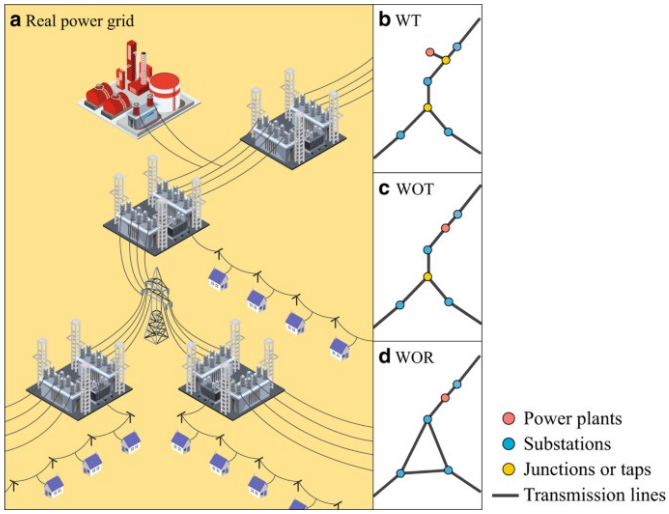

Figure 3.2: Three ways to abstract a power grid into a network: 'with tap' (WT), 'without tap' (WOT), 'without tap reduced' (WOR). From Kim et al. (2018, Figure 1).

Another question is how to model different voltage levels. One option is to consider every voltage level as a single network, and the complete grid as a multilayer network consisting of the different voltage levels. The other option is to take the entire grid as a single network. The different approaches are visualized in Figure 3.3. It turns out that this choice has an impact on whether networks are small-world: Espejo et al. (2018, p. 391) report that for 15 different European grids studied, all of them are small-world when the two voltage levels (220 kV and 400 kV) are combined in a single network. But when these voltage levels are analyzed as independent layers, there are some that fail to meet the threshold for small-worldness.

Finally, another point of concern is how to model high voltage pylons that carry multiple separate power groups. If each group is mapped as a separate line, they will show up as multiple edges in the network, and it will increase the average degree. If not all pylons carry the same amount of groups, this can also change the shape of the degree distribution.

Inspired by Kim et al. (2018), we follow a middle way: we both try to make a dataset that is as detailed as possible, but also implement reduction methods to create a reference network format which we can use to compare networks from different sources. Specifically, this means we model the network as one single network, where the voltage layers are connected by transformers (a special type of edge). Plants are also encoded as nodes, in principle with one node per 'generating unit', which for thermal plants is often a turbine, with plants possibly consisting of multiple turbines. We call foreign substations 'subnets', since they represent an entire foreign subnetwork. We include parallel circuits, which we encode as parallel edges between the same nodes, that can be distinguished by specifying a 'color' for every circuit (a common practice also for distinguishing physical transmission lines). We add junction and taps where appropriate. Often these junctions and taps refer to specific high voltage pylons, but this is not the case in general, and junctions do not need to represent physical locations or connections. They have three uses: they help in approximating circuit length by adding intermediate stops; they improve graphical representation, making it easier to follow the path of a circuit; and they can simplify data input when over time only the endpoint of a node changes, but not the intermediate steps. The difference between

[2]This type of node classification is common, but might occur under different names. For example, Albert et al. (2004) calls them generators, distribution stations, and transmission substations respectively.

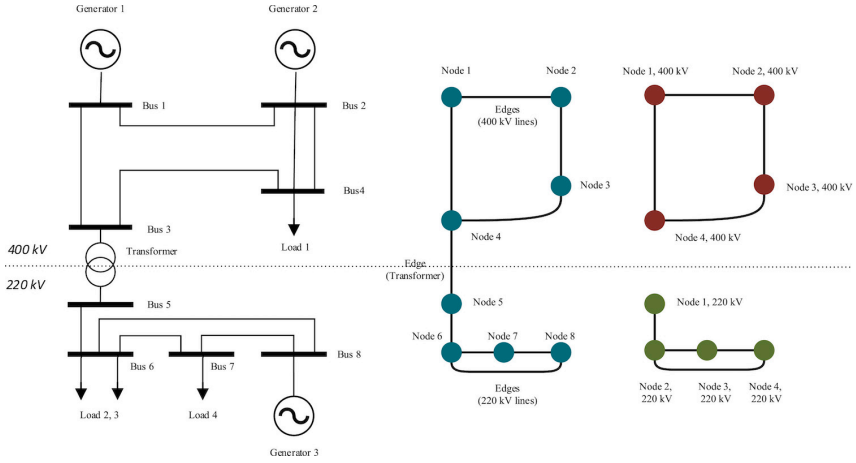

Figure 3.3: Modeling different voltage levels: as a single network or as multiple independent layers. On the left: a diagram of a power grid. On the right: two versions of a network abstraction of this power grid – as a single network with 8 nodes, and as two networks with 4 nodes each. From Espejo et al. (2018, Figure 1).

a junction and a tap is that a junction should always connect precisely 2 edges of the same color, while a tap can connect more than 2 edges of the same color. This is needed in situations where a substation is electrically connected to an existing line between two other substations. In this way, one circuit can connect more than two substations.

The *reference version* of a network is created as follows: we remove the node representing plants, and reduce junctions and taps by replacing the circuits with one edge connecting the appropriate substations (using a so-called star-mesh conversion). The remaining nodes are then only substations and subnets. We condense parallel edges into one, so that the graph becomes simple. We also split nodes that are connected at multiple voltages into multiple nodes with transformers in between, so that each node has its voltage specified. An example of this process is visualized in Figure 3.4.

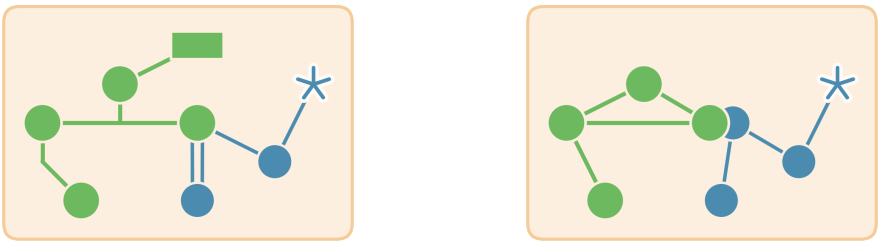

Figure 3.4: Example of a network (left) and its reference version (right). Creating a reference version ensures that calculations on networks from different sources can be compared to each other. The colors indicate different voltage levels, the rectangle is a power plant, and the star symbol is a foreign subnet. Between the overlapping nodes is a transformer.

3.2 Assessing synthetic network models

There are many synthetic network models to consider (see Table 2.2), but the most important ones are those which have a temporal and spatial output: they generate a sequence of networks throughout time and positioned in space. Based on my literature search, only the models from Deka et al. (2017) and Mei et al. (2011) meet these criteria. Due to time constraints, we will confine the analysis to the model from Mei et al. (2011). Although there are a number of tweakable parameters, the fit appears decent enough that we simply continue with the suggested parameters.

3.3 Power flow

To calculate the power flow, we need to know the networks topology, the electrical parameters of the nodes and edges, the loads of the substations and the generation of the power plants, and we need a solver which can calculate a solution to the optimal power flow problem. Because it is a time-consuming process to gather the required data, we will only calculate the power flow on the Dutch network, and for 2020 since that is a recent year for which we can find all the required data. The network topology follows from our network dataset. For the electrical parameters and the load and generation, we use external data from TenneT, ENTSO-E, and the Dutch statistical bureau CBS (see Appendix A). As solver, we use GridLAB-D, an open source simulation tool developed at SLAC (Chassin et al., 2022).

Due to time constraints, we use the average load per substation and generation per power plant over 2020. Since we are interested in the vulnerability of the network, we want to remove nodes from the network while the network is under 'extreme' conditions. To simulate this, we lower the capacities of the lines to the minimum possible so that there is still a solution when no nodes are removed. This means that when a node is removed, it is more likely to result in lines that are over capacity. When lines are over capacity, we iteratively reduce the load at substations until we find a solution where the line capacities are respected again. Specifically, we find the substation whose voltage has dropped the most relative to its nominal voltage, and reduce its loads by 20%. Although this is a crude approximation of the extreme conditions and the behavior when nodes are removed, it does indicate which nodes are most important for the networks reliability, and allows use to compare it to the topological vulnerability node-by-node.

3.4 Testing for preferential attachment

To test for preferential attachment behavior in the growth of the network, we assume that there is a function f such that the probability of a new node connecting to an existing node of degree x is proportional to $f(x)$. If there is *no* preferential attachment, then the degree of a node has no influence on whether a new node will connect to it, so $f(x) \propto 1$. On the other hand, if there is *linear* preferential attachment, such as in the scale-free networks generating model from A.-L. Barabási and Albert (1999), we have $f(x) \propto x$. There are different ways to estimate the shape of such a function f from data on empirical network growth (A. L. Barabási et al., 2002; Jeong et al., 2003; Newman, 2001; Pham et al., 2015). The simplest way, inspired by Newman (2001), is to count how many times a new node connects to a node with degree x, and compare it to the expected number of connections if there was no preferential attachment. Then, by dividing we get a ratio as estimate for f:

$$\hat{f}(x) = \frac{\#\text{ new nodes connected to node of degree } x}{\mathbb{E}\,\text{connections to node of degree } x \text{ without preferential attachment}}.$$

We use $m(t)$ to denote the number of edges in year t, $n(t)$ the number of nodes in year t, and $n_x(t)$ for the number of nodes of degree x in year t. As time resolution, we use one year, so every year we determine what the new nodes are, to which existing nodes they connected, and what the degree of those nodes was. If we assume that new edges are only formed between an existing node and a new node, then for every degree x we can calculate our estimate as:

$$\hat{f}(x) = \frac{\sum_t \#\text{ nodes added in year } t+1 \text{ that connected to a node which had degree } x \text{ in year } t}{\sum_t (m(t+1) - m(t)) \cdot n_x(t)/n(t)}.$$

To compare this to a scenario with linear preferential attachment, we note that in that case the probability of a new edge connecting to a specific node of degree x is given by

$$\frac{x}{\sum_{i \in V} k_i(t)} = \frac{x}{2\,m(t)},$$

since summing the degrees of all nodes is the same as counting every edge twice. And since there are $n_x(t)$ nodes of degree x in year t, we see that in a linear preferential attachment scenario:

$$\hat{f}(x) = \frac{\sum_t (m(t+1) - m(t)) \cdot n_x(t) \cdot x/(2\,m(t))}{\sum_t (m(t+1) - m(t)) \cdot n_x(t)/n(t)}.$$

If we only consider one time step, this is equal to

$$\frac{x/(2m)}{1/n} = \frac{x}{2m/n} = x/\overline{k}.$$

Chapter 4

Results

4.1 The dataset

The resulting dataset covers the Dutch transmission grid from 1931 to 2023 (and also including some components under construction up to 2026).[1] It consists of 685 nodes and 1653 edges. Of the nodes, there are 399 regular substations, 118 plants, and 17 foreign subnets. There are also 121 junctions and 30 taps. Of the substations, there are 58 commercial substations, which connect to a private distribution network. Of the edges, 85 are transformers, and the remaining 1568 are transmission lines (no distinction is made between cables and overhead lines). This is the full version of the network, with all historic components, and including parallel lines. Snapshot of the networks evolution are show in Figure 4.1 and a visualization of the full version is shown in Figure 4.2.

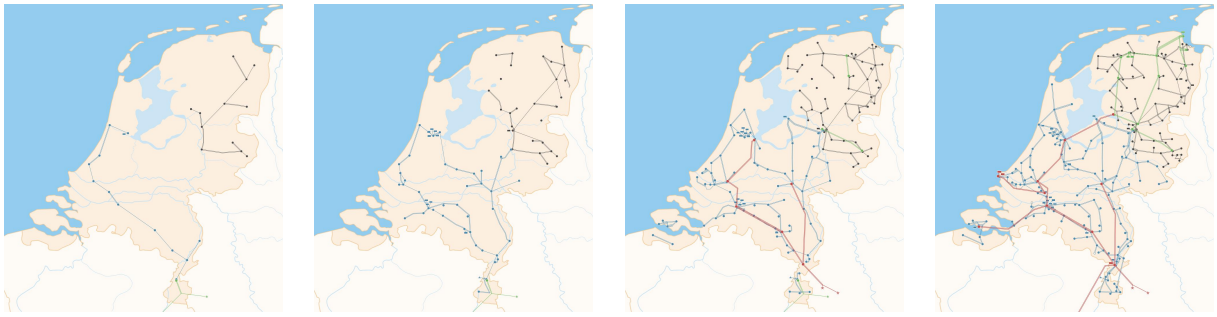

(a) 1950 **(b)** 1960 **(c)** 1970 **(d)** 1980

(e) 1990 **(f)** 2000 **(g)** 2010 **(h)** 2020

Figure 4.1: Snapshots of the state of the network per decade.

[1]The dataset will be published within the github.com/slacgismo organization under an open source license.

Figure 4.2: Visualization of the complete dataset. The network has never existed in this state, since this visualization also includes substations and lines which have been dismantled at some point.

4.2 Evolution of network characteristics

The development of a number of characteristics is visualized in Figures 4.3 to 4.8, for both the Dutch and Hungarian transmission grids. From now on, all reported characteristics have been calculated on the reference versions of the graphs, as defined in Section 3.1.2. This means that we only consider substations and subnets as nodes, reduce junctions and taps, and condense parallel edges resulting in a simple graph.

In Figure 4.3 and 4.5, we see that both networks share an initial rapid growth from the 1950s to the 1970s. After that period, the growth rate is reduced and is approximately linear. The number of nodes and specifically the number of edges of both networks are remarkably similar over time, considering that the two networks are different in both spatial size (the land area of Hungary is more than twice that of the Netherlands), population size (9.7 million people in Hungary versus 17.8 million in the Netherlands), and economic and historical context. The evolution of the average degree follows directly from the number of nodes and edges, and is also given in Figure 4.5. From the 1970s onwards, the average degree is stable for both networks (around 2.9 for the Netherlands and 2.6 for Hungary). Figure 4.4 shows that much of the growth has occurred in the 120/150 kV layer, with the 220 kV and 380/400 kV layers taking up a relatively small and constant share of the total amount of nodes. Only in recent years have the 110 kV and 380 kV layers of the Dutch network started growing again, while in the Hungarian network the 100 kV layer has seen continuous shrinking.

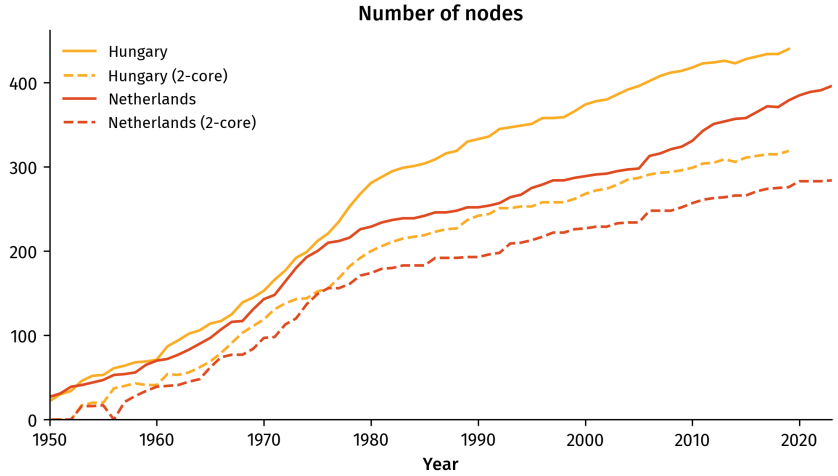

Figure 4.3: Number of nodes over time, compared between the Dutch and Hungarian networks. Included node types are substations and subnets, while taps, and junctions are reduced, and plants are filtered out. The 2-core is the maximal subgraph such that all nodes have degree at least 2.

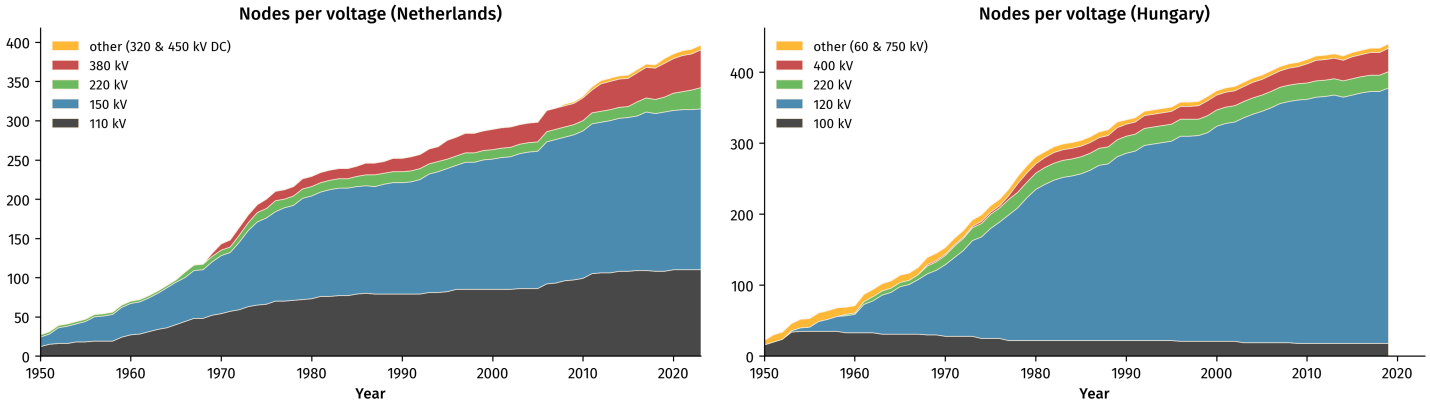

Figure 4.4: Number of nodes per voltage level over time. Note that the Hungarian voltage levels are similar but not exactly the same as those of the Dutch network

In Figure 4.6 we see that the distance and diameter of both networks share a similar evolution too, with the average distance stabilizing in the 1970s around 8. This happened while both networks were growing,

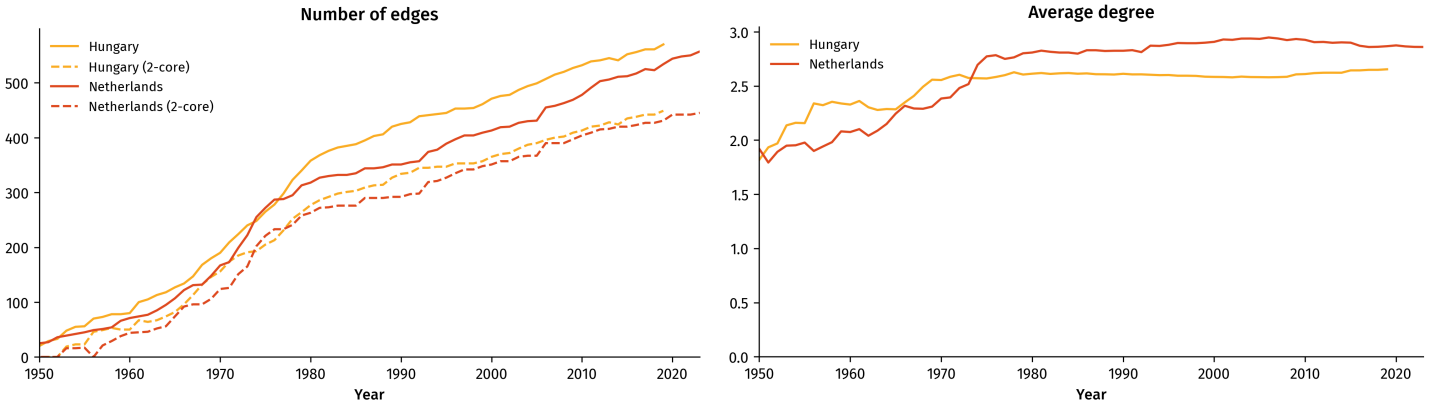

Figure 4.5: Number of edges and average degree over time, compared between the Dutch and Hungarian networks. This includes edges which denote transformers. The degree is the number of outgoing edges of a node. Since our graph is simple, there are no parallel edges, and the degree is the same as the number of neighbors of a node.

and since for random networks you expect that the average distance increases with increasing network size, this is an indication that the network shows small-world properties. This is confirmed by Figure 4.7, showing that for both network the small world coefficient crosses the threshold of 1 already in the 1960s. The difference in the small world coefficient is mainly explained by the larger local clustering coefficient of the Dutch network.

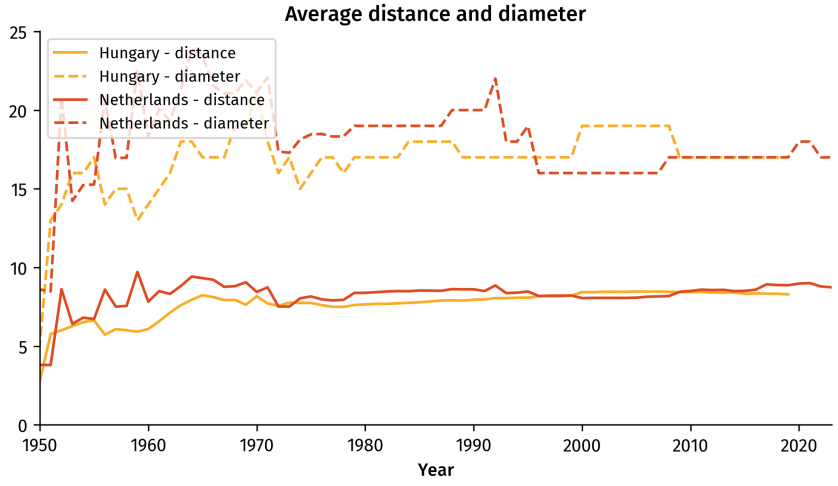

Figure 4.6: Average distance and diameter over time, compared between the Dutch and Hungarian networks. This is calculated using the unweighted topological distance: the smallest number of steps required to move from one node to another. The diameter is the maximum distance between two nodes, so the length of the longest path in the network.

4.2.1 Degree distribution

Figure 4.8 compares the degree distributions of both networks over time. We see the maximum degree is increase over time, ending at 11 for the Dutch network and 9 for the Hungarian network. The 2020 degree distribution of the Dutch network shows up as an almost straight line on the log-plot, indicating that the degree distribution is exponential. For the Hungarian network, the 2020 degree distribution starts out as a straight line, but tapers off around degree 7. This indicates that the Hungarian substations have a lower number of maximal connections, and that after this point more connections are unlikely.

Combining all observations leads to the impression that after the initial growth from the 1950s onwards the networks became 'saturated' in the 1970s, and that further growth has mainly occurred to serve increasing and new loads, without drastic changes to many network characteristics.

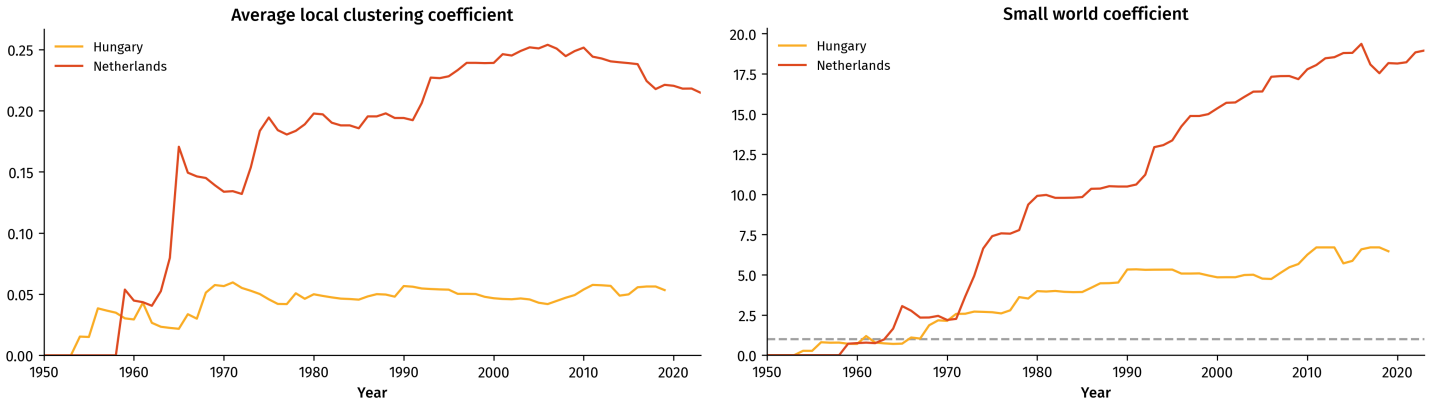

Figure 4.7: The average local clustering coefficient and the small world coefficient over time, compared between the Dutch and Hungarian networks. The local clustering coefficient of a node is the share of its neighbors that are also connected among each other. The small world coefficient is calculated by comparing the average distance and clustering coefficient to that of a random network of the same size.

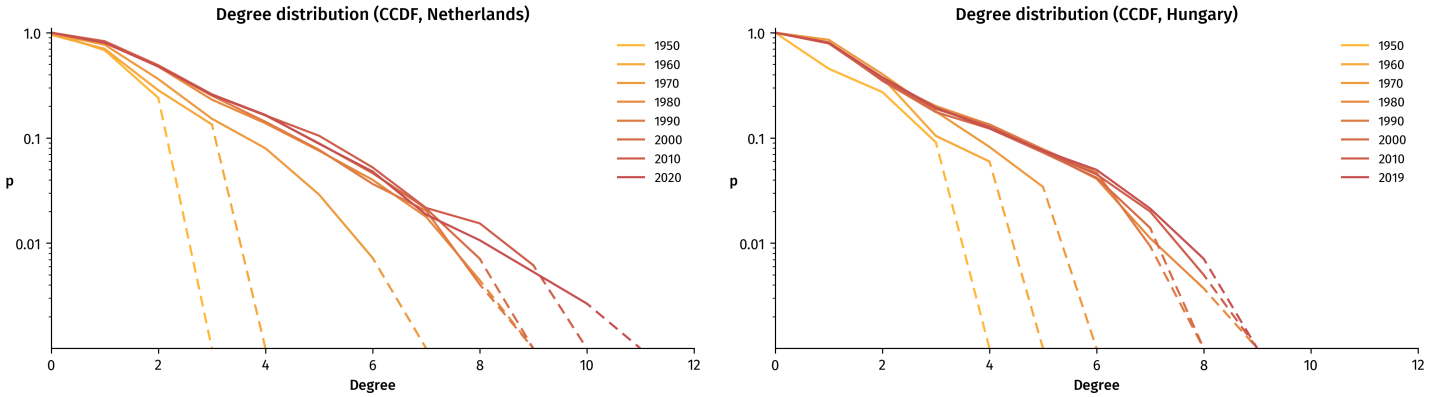

Figure 4.8: The distribution of node degrees over time. We calculate the complementary cumulative distribution function (CCDF), which is defined as $\mathbb{P}(k > x)$ where k is the degree (see Section 2.2). So the value for $x = 0$ is $\mathbb{P}(k > 0) = 1 - \mathbb{P}(k = 0)$, the value for $x = 1$ is $\mathbb{P}(k > 1) = 1 - \mathbb{P}(k = 0) - \mathbb{P}(k = 1)$, etc. Note that the y-axis is logarithmic. For the maximum degree k_{max} we have $P(k > k_{max}) = 0$, which we can not plot on a logarithmic axis. Instead, we draw a dashed line to the x-axis to indicate its value.

4.3 Growth processes in real and synthetic networks

4.3.1 Testing preferential attachment

To test to which degree the networks exhibit preferential attachment, we calculate the ratio between the times a new node connected to an existing node of a certain degree versus the number of times this would have happened if there was no preferential attachment, as explained in Section 3.4. The results for the Dutch and Hungarian networks are given in Figure 4.9. We see that both networks exhibit preferential attachment, with ratios above 1 for higher degree nodes that are more likely to receive new connections. For the Hungarian grid this is especially pronounced, with for the higher degrees ratios above even linear preferential attachment. The effect for the Dutch grid decreases for degrees above 8, which is expected since the number of incoming connections a substation can have is bound to space limits. Note that the variation in ratios becomes high for higher degrees, since there are only a limited number of these nodes so only a small number of new connections can significantly influence the ratio. In general, the ratio should be 0 for nodes of the maximum degree, since they can not have received extra connections (which would increase their degree). This is not the case for the Hungarian grid, because it has happened that nodes with the maximum degree of 9 have in the same year received a new connection, but also lost an existing connection.

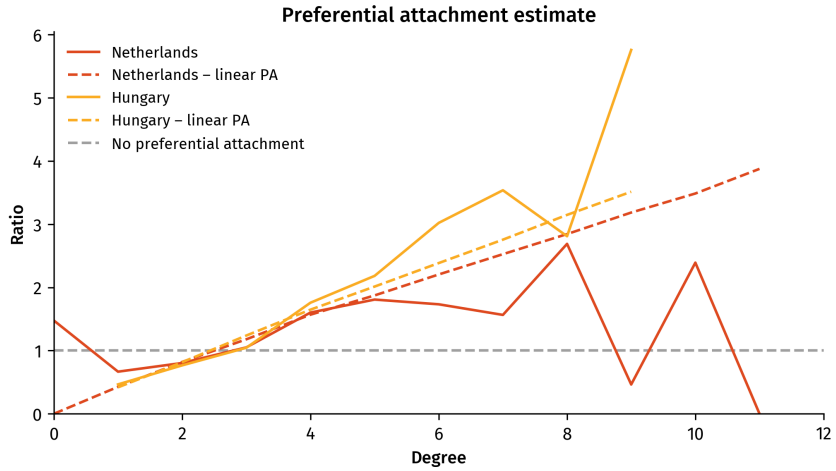

Figure 4.9: Estimate of preferential attachment ratios, calculated by comparing the number of new connections to nodes of a certain degree to the scenario where there would be no preferential attachment, so all nodes are equally likely to receive new connections. If there is no preferential attachment, the ratio is 1, while in the case that there is linear attachment (so probability of a node receiving a new connection is proportional to their degree) the expected ratio is roughly linear in the degree.

4.3.2 Comparing synthetic network generators

As explained in Section 3.2, we chose the synthetic network model from Mei et al. (2011) as a simple model which can generate synthetic transmission grids. We performed 20 different simulation runs with different random initial conditions. We start the simulation in 1950, and run it for 70 years until 2020. The results of these simulations are compared to the Dutch and Hungarian networks on a number of characteristics in Figures 4.10 to 4.13. From the simulation algorithm, we expect a linear growth in the number of nodes and edges, and this is confirmed by Figure 4.10. Even without changing the suggested parameters, the fit – although linear – is quite good for both networks. However, if we look at the 2-core of the networks, we see that the 2-core of the simulation runs is much smaller, both in the number of nodes and the number of edges. This indicates that there are more leaf nodes with degree 1 in the simulated networks, and that simply attaching new nodes to the nearest existing substation leads to fewer ring structures where all nodes have degree at least 2.

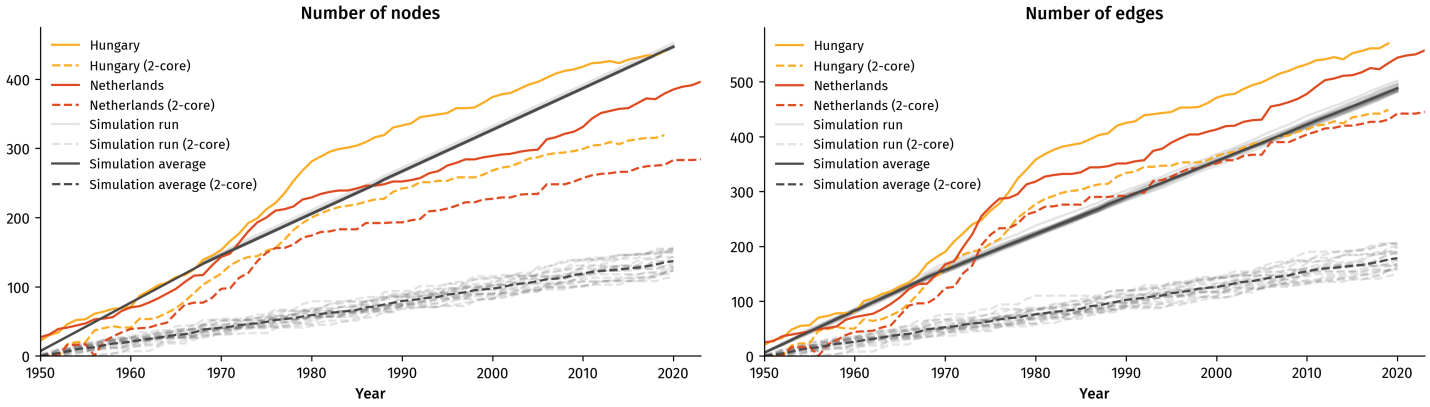

Figure 4.10: Number of nodes and edges compared between 20 simulation runs of the synthetic network generators and the real-world networks.

In Figure 4.11, we see that the average distance of the simulations starts out relatively low, but takes longer to stabilize than the real-world networks, and also stabilizes at a slightly higher value around 11. On the other hand, the small-world coefficient of the simulated networks on tracks that of the Hungarian network very well. We see that the simulated networks all become small-world networks.

From the evolution of degree distributions and the for the final state to those of the Dutch and Hungarian networks shown in Figure 4.12, we see that the simulations have more nodes with lower degrees. Although

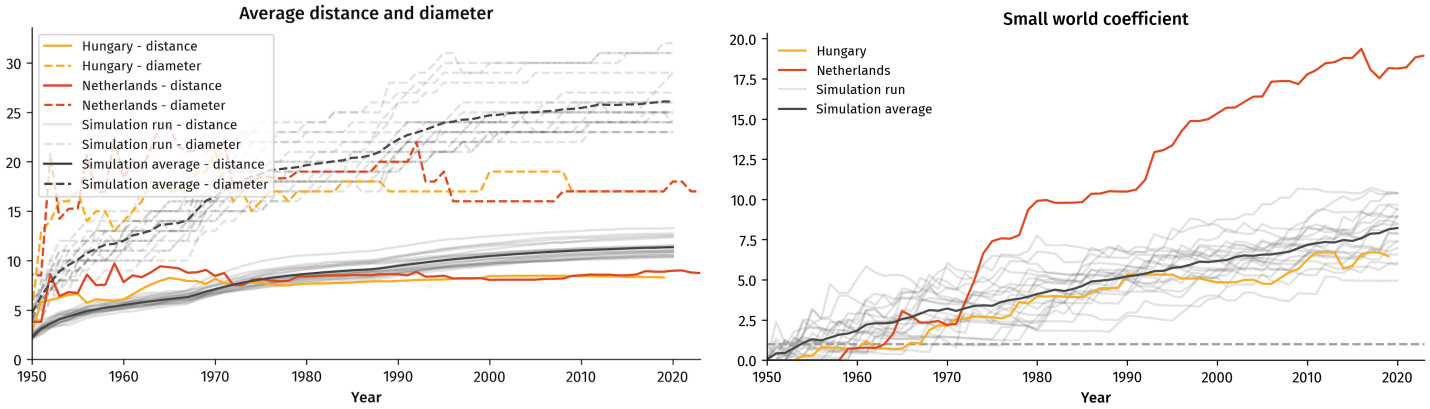

Figure 4.11: Average distance, diameter, and resulting small world coefficient compared between 20 simulation runs of the synthetic network generators and the real-world networks.

it evolves to become closer to a line on the log-plot, it does seem to taper off a bit stronger and sooner than the real-world networks, so it is less clear that this degree distribution also becomes an exponential distribution. From the simulation runs, we do see that the variation is relatively large, with one network ending up with a maximum degree of 12, higher than what we have seen in the real-world networks.

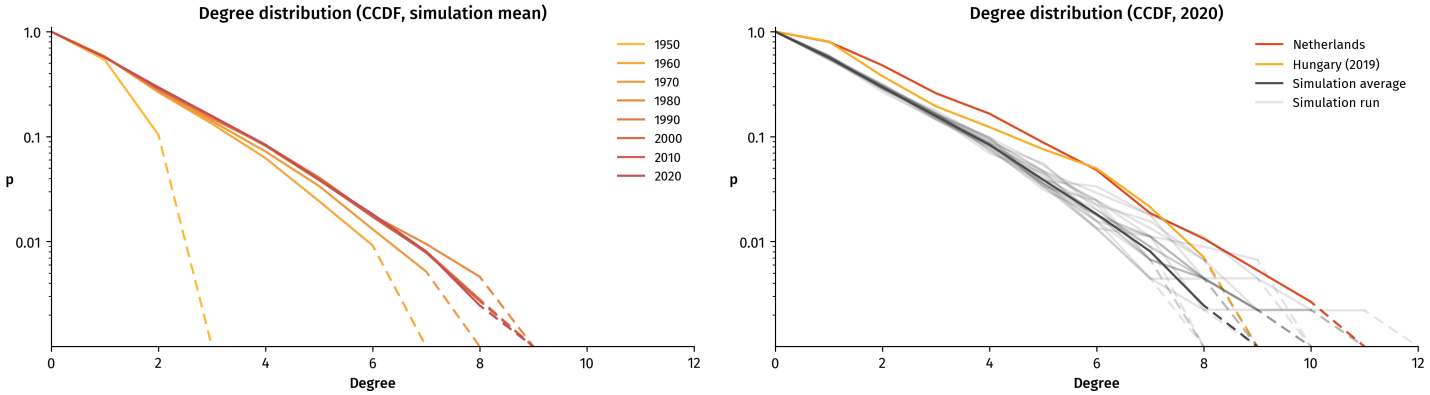

Figure 4.12: Evolution of the degree distributions (plotted as complementary cumulative distribution function, see Section 2.2.3) for the average of 20 simulation runs, and comparison of the final degree distribution between the simulation runs and the real-world networks.

Finally, we also calculate the preferential attachment estimate for the simulation runs. In the synthetic network algorithm, there is no preferential attachment specified, so we expect to find ratios around 1. This is confirmed by Figure 4.13, showing that up to and including degree 6, the average ratios are very close to 1. For higher degrees, the variation between simulation runs and the fluctuation of the resulting average is much higher. This is because the number of nodes with higher degrees is much lower, so one connection more or fewer can have a large impact. Even then, the ratios of the average stay below the dashed line which indicates the expected value when there is linear preferential attachment.

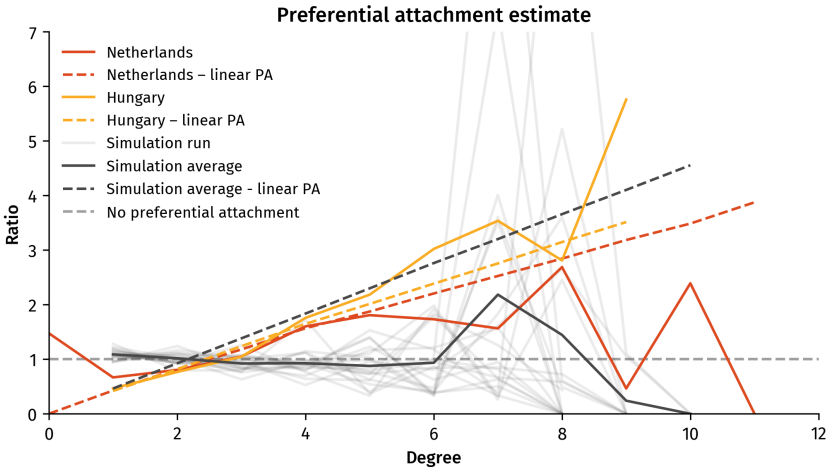

Figure 4.13: Comparison of the preferential attachment ratios estimates between the 20 simulation runs and the real-world networks. Ratios around 1 indicate that there is no preferential attachment.

4.4 Vulnerability analysis

4.4.1 Topological analysis

To quantify the topological vulnerability, we calculate the efficiency of the networks and the maximum drop in efficiency if a node is removed. The results are given in Figure 4.14. We see that the efficiency for both the Dutch and the Hungarian networks stabilize after the 1970s, at around 0.15. Since the efficiency is the average of the inverse distance between nodes, we can expect that the inverse of the efficiency is of the same order as the average distance. And indeed, given that $1/0.15 \approx 7$ and that the distances for the Dutch and Hungarian networks stabilized around 8, this is quite close. For the maximum drop in efficiency, we see a more fluctuating and different pattern until the 1970s, but this also stabilized around 10% for the Dutch network and 5% for the Hungarian network. This parallels the conclusion from Hartmann (2021) who notes for the Hungarian network that "[t]his suggests on the one hand that the elements most important for security have been installed before [the 1970s], but on the other hand it implies that grid development of the last 40 years could not significantly contribute to this aspect." It is interesting to see in this regard that the topological vulnerability of the Dutch network is roughly double that of the Hungarian network, even though the efficiencies are similar. This would indicate that the Hungarian network has found a more robust topology than the Dutch network. This is especially noteworthy because Hartmann (2021) finds a negative correlation between the clustering coefficient and the vulnerability, but the Dutch network has a higher clustering coefficient than the Hungarian network – the opposite from what you would expect based on the correlation.

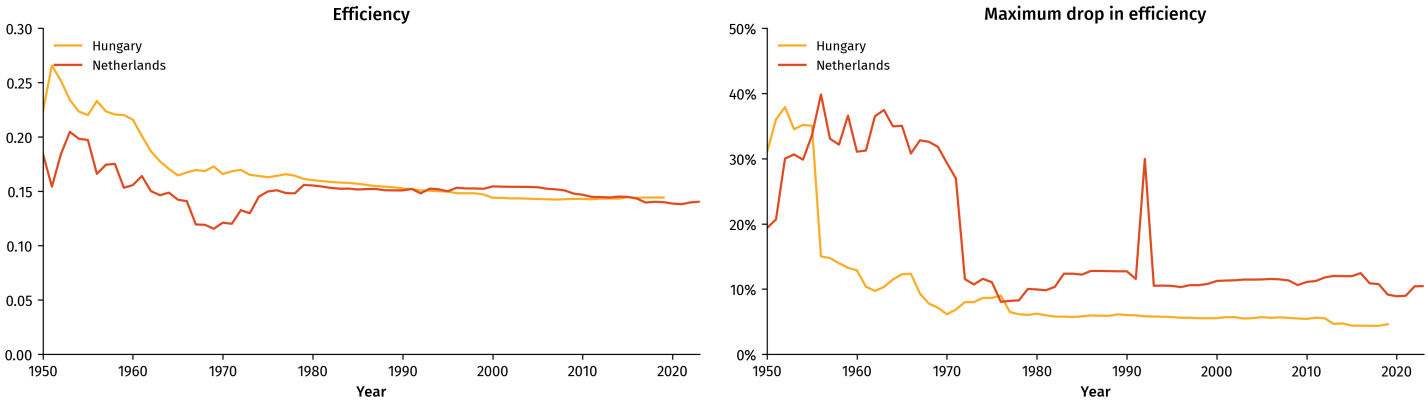

Figure 4.14: The evolution of the efficiency and maximum drop in efficiency after removing a node, compared between the Dutch and Hungarian networks.

Figure 4.14 shows a strong peak for the Dutch vulnerability in 1992. To understand where this peak

comes from, we map the Dutch networks of 1991 and 1992 in Figure 4.15, where we scale the sizes of the nodes by the efficiency drop after removal of that node. In 1991, there were multiple nodes with a high topological vulnerability, mainly on the 380 kV ring, and at the connection points of transformers. In 1992, we see that the substation of Ens in the northern part of the Netherlands sees a strong increase in vulnerability. This is because in between 1991 and 1992, the transformer connecting 150 kV layer (blue) and the 110 kV layer (black) in the north was removed. The transformer between 220 kV (green) and 380 kV (red) in Ens then became the only substation with which the northern part of the network was connected to the rest of the country, and hence became very important for the efficiency of the network. This bottleneck was removed in 1993 by the addition of a transformer between the 110 kV and 380 kV layers, in the eastern part of the country.

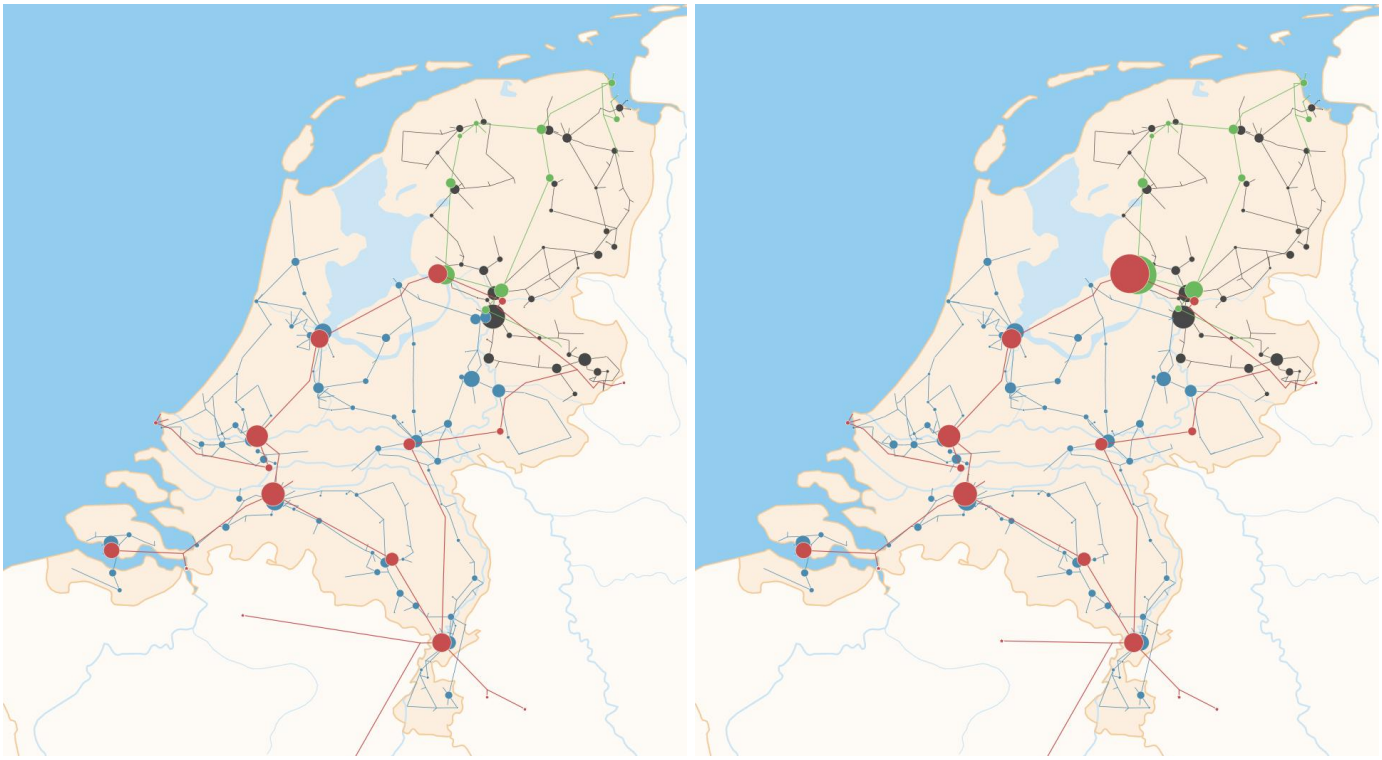

(a) 1991 **(b)** 1992

Figure 4.15: The Dutch network in 1991 and 1992, where the nodes have been scaled to their topological vulnerability, i.e. the drop in the networks efficiency if they would be removed from the network.

We also compare the efficiency and vulnerability of the real-world networks to the synthetic networks in Figure 4.16. The efficiency of the simulated networks starts out high, but in 20 years drops to a similar level as the Dutch and Hungarian networks. Striking however, is the difference in topological vulnerability: the average vulnerability of the simulations stays around 40%. This shows that even though we have seen that the synthetic networks resemble real world networks in some important characteristics, the networks are much more vulnerable to disruptions.

4.4.2 Power flow analysis

The results of the power flow simulation for the full network are visualized in Figure 4.17. We see that the 380 kV backbone plays in important role in the transmission of electricity from the plants near the port of Rotterdam in the southwestern region, and from the plant in the southeastern part of the country. Locally, although the network structures are meshed, small quasi-radial subnetworks seem to emerge on lower voltages. The imports over German connections serve as important sources for the eastern part of the network.

With the simulation on the complete network as a base line, we then recalculate the flow after removal of one node. In many cases, especially for leaf nodes, the only load loss that occurs is the load of the node itself. In some extreme cases, the solver can not find a power flow anymore, and all load is dropped. The load losses and correlations with the topological efficiency drop is given in Figure B.1. We see that

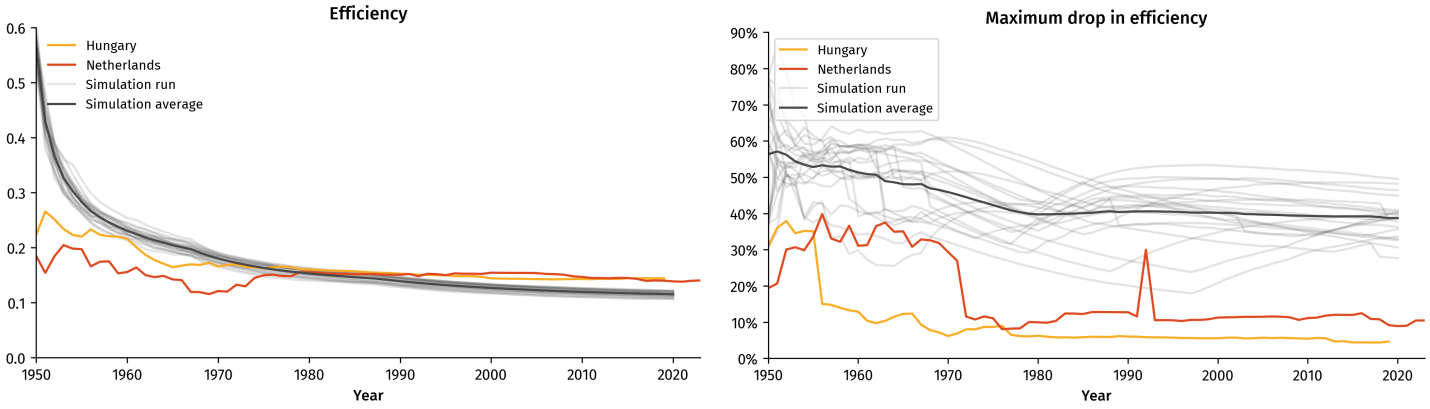

Figure 4.16: Comparison of the efficiency and topological vulnerability between the 20 simulation runs and the real-world networks.

– surprisingly – in many cases where the network becomes unsolvable (load loss around 6000 MW), it is a node from the 110 kV layer that has been removed. If we ignore the cases where (part of) the network becomes unsolvable, and zoom in on the cases where the loss of load is lower (the right subfigure), we see that it is hard to derive a strong correlation between the topological vulnerability and the vulnerability of the power flow simulation. Many nodes for which there is a significant drop in topological efficiency, can be removed from the network without any other loads having to be shed.

Figure 4.17: Result of solving the optimal power flow for 2020. Node sizes are proportional to their load or generation, and widths of the edges are proportional to the amount of power transported over that edge. In the solution, not all the power generated by a plant is always transported over a line, when this is not required to satisfy the loads. This is the reason some power plants look to be disconnected while still producing electricity.

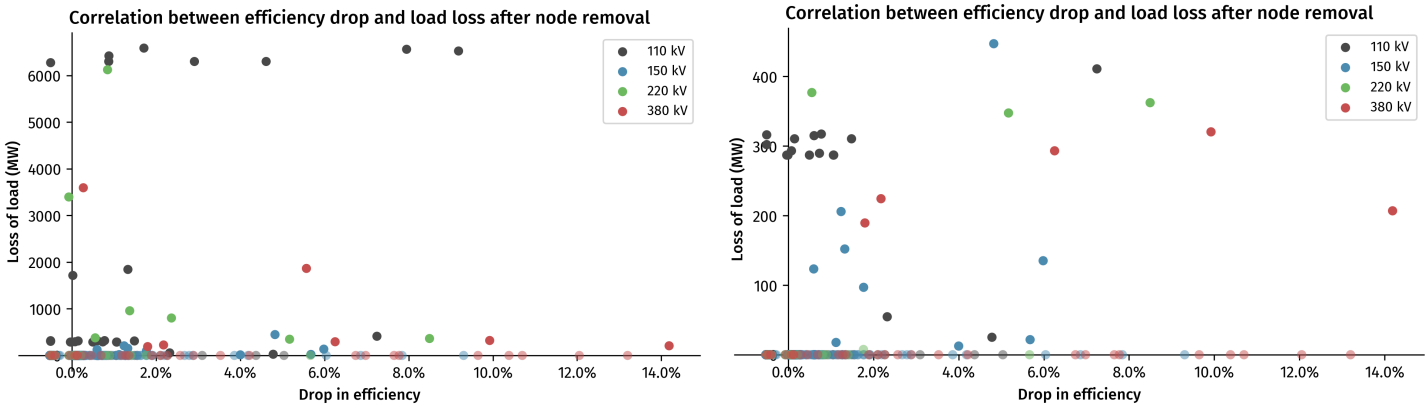

Figure 4.18: Correlation between the efficiency drop and the loss of load when a node is removed. The right figure is the zoomed in version of the left figure. Nodes with a negligible amount of load loss have been made slightly transparent, so they can be discerned when they are stacked with other nodes.

Chapter 5

Discussion

5.1 Data quality

The dataset of the Dutch grid is based on historical maps, combined with recent data from the transmission system operator TenneT on the build years of existing substations (TenneT, 2022c). The current state of the network is well documented, with high resolution maps showing the trajectory of different circuits, and high quality secondary sources. However, after comparing the build years supplied by TenneT to the historical maps, we saw that not all the build years of substations match the first occurrence on the yearly maps. For many substations and lines, we have been able to find the correct build year, but due to time constraints this was not possible to do for all years. Also, historical lines and substations which have existed in the past, but have been dismantled, can only be inferred from the historical maps. For the recent decades, we have been able to add these dismantled components to the dataset, but also due to time constraints the dataset might not be complete for the first decades. However, our main conclusions derive from the post-1970 network structure, for which we are confident that the accuracy of the dataset is high enough, so this should not influence our results in a significant way.

5.2 Sensitivity to network construction parameters

As we noted in Section 3.1.2, there are many ways to abstract physical electrical grid into network representations. For our calculations, we have worked with a reference version of the networks. However, if we use the full version, which includes among others parallel circuits, this can significantly influence the degree distribution, since nodes generally have more connections in the full version. Also, some authors do not encode transformers between voltage layers as a separate edge, and instead use one node two represent the different voltages of the same substation. This will also increase the degree for these nodes, since they have connections from multiple voltage layers. The effect for these choices on the degree distribution of the Dutch network is visualized in Figure 5.1. We see that the full version of the dataset has nodes of a much higher degree. When we reduce the transformers, there are even two nodes (Diemen and Geertruidenberg) with a maximum degree of 37. This shows that it is very important to create a reference version when comparing networks, and also to specify the steps taken to derive this reference version when reporting numerical results.

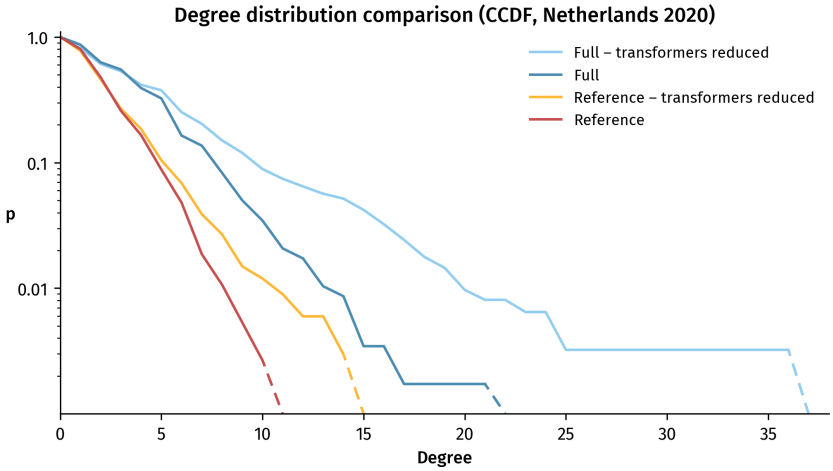

Figure 5.1: Comparison of the degree distribution between four versions of the same Dutch network in 2020.

5.3 Choice of metrics

For the vulnerability analysis in Section 4.4.1, we used the unweighted efficiency to calculate the topological vulnerability. As explained in Section 2.5.1, there is also the *weighted* efficiency metric which compares the weighted distances in a network to the optimal distances if a network was fully connected. If we take the length between nodes as the weight of an edge, we redo the efficiency and vulnerability calculations. The results are shown in Figure 5.2. Note that a value of e.g. 0.80 means that the average inverse distance between nodes is 80% of the inverse direct distance between nodes. What is surprising, is that the Dutch weighted efficiency shows much more fluctuation than in the unweighted efficiency (see Figure 4.14). We saw before that the removal of a transformer in 1992 caused a bottleneck which increased the unweighted vulnerability. Here, it shows up as a strong dip in the weighted efficiency, much more noticeable than the dip in unweighted efficiency in 1992. So apparently there was a short alternative path around this transformer in number of hops, but this detour made this path much longer in terms of physical length. This can be explained by the fact that a detour in the 380 kV layer only needs a small number of steps to travel a long distance, since the average distance between substations in that layer is high.

In the weighted vulnerability, we also see some striking differences to the unweighted vulnerability: it takes until 1993 – instead of the 1970s – for the Dutch vulnerability to stabilize, but when it does, it is at a very similar level to the Hungarian vulnerability. So the transformer added in 1993 had a much larger effect on the average distance between nodes, than on the average number of steps between nodes, and was essential in bringing down the weighted vulnerability. This difference also illustrates that it is important to consider which vulnerability metric to choose. Simple topological measures have their use, since they are easy to calculate and do capture essential characteristics of the network, but they might miss noteworthy developments in characteristics unrelated to the topological distance.

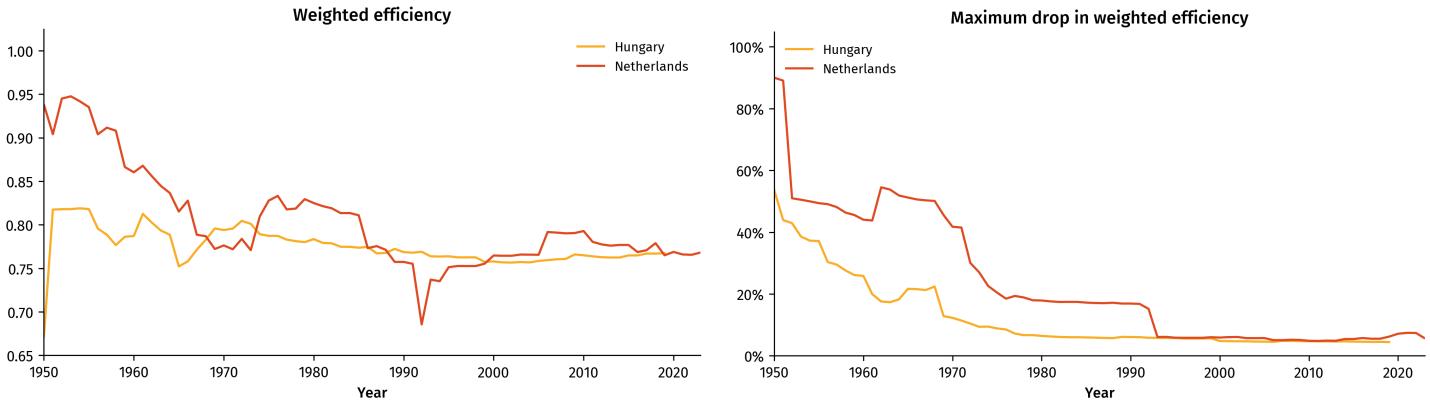

Figure 5.2: Topological efficiency and vulnerability using the *weighted* version of network efficiency. As edge weights, we used the (geometric) length between two nodes. The weighted efficiency is normalized by dividing by the optimal efficiency where the network is fully connected, so that the efficiency is always between 0 and 1. This allows for comparison between networks of different sizes.

5.4 Limitations of the power flow analysis

Without accurate load shapes for every substations with a high time resolution, it is very difficult to calculate the precise load flows and also understand at which point in time the network is closest to its capacity. We have tried to overcome this problem by using the yearly average flows and reduce the line capacities until the network is almost at capacity, but this is a crude approximation. One important drawback of this approximation is that failures can become large under specific 'extreme' conditions: either a load peak, or a non-standard distribution of load and generation over the network. Even though these extreme conditions can be rare, they could determine the bottleneck for a networks vulnerability. We also only consider taking out a whole substation, but a more detailed analysis – which also requires more data on the precise setups of components, e.g. the number of transformers in a substation – where specific subcomponents such as transformers or single lines fail, can provide more realistic failure scenarios. The problem is that these detailed analyses are hard to carry out for multiple networks at the same time, making comparisons between networks difficult.

Chapter 6

Conclusion

We have seen that the Dutch and the Hungarian network have a similar evolution for a number of important network characteristics. After an initial rapid growth phase between the 1950s and 1970s, the networks matured and many characteristics stabilized. The topological vulnerability of the Dutch network has stayed higher than that of the Hungarian network, although if you consider the weighted vulnerability, the Dutch network dropped to a similar level after the completion of the first 380 kV ring. Both networks have shown strong preferential attachment, which leads to an exponential degree distribution, likely due to the physical limit to a substations degree. Network characteristics such as the degree distribution are strongly dependent on the way in which networks are constructed and represented, so a uniform reference format is essential to allow for comparison between networks. The power flow analysis showed that the flow solutions can be very sensitive to node removal, although we saw little correlation between the topological and flow-based vulnerability.

The synthetic network generator which we studied is simple, but still fits well to the real-world evolution on a number of characteristics. However, in terms of the vulnerability, it did not capture the observed drop in vulnerability, and vulnerability stayed high. This illustrated that care is required when using synthetic network generators, and that only after validation on the property of interest, can they be safely used. Also, due to the lack of preferential attachment in the growth mechanism, the degree distribution was concentrated on lower degrees compared to the Dutch and Hungarian distributions.

6.1 Future work

There are many ways to build on our research. First, there are a number of ways to improve and validate synthetic networks using the dataset we have created: building in preferential attachment and changing the algorithm to create more ring structures are two clear steps. Different types of metrics could also clarify the gap between real-world and synthetic networks. An interesting approach is to consider not just the distance between nodes, but specifically the distance between source and load. This distance – and loads – will decrease when more distributed energy resources are connected to the grid. It would also be possible to find a hybrid between purely topological and power flow based methods, by using network flow measures such as the maximum flow between two points, taking into account edge capacities. If a synthetic network generator can be found which is validated on a number of network characteristics, running the simulation into the future could be an interesting way to generate possible network scenarios.

The power analysis can be improved by more accurate load shapes with a high time resolution. In our approach, we assumed that the loads would decrease to match line capacities. However, the most catastrophic grid failures result from lines that become disconnected after their line capacity has been exceeded, and the sudden rerouting of the existing flow also overloads nearby lines, leading to a cascade of line failures (Nesti et al., 2018). It would also be very interesting to extend the power flow analysis to historical networks, although there extrapolation of the load shapes is required.

Finally, a promising avenue is to consider the electrical network as just one layer in a multi-layer network. The other layers can be communication networks (Buldyrev et al., 2010), transportation networks, cyber-physical networks (Brummitt et al., 2013), or political networks that represent for example local energy

communities with distributed resources. Then, we can consider the co-evolution of these networks, where growth or changes in one layer of the network induces changes in the other layers.

Chapter 7

Bibliography

Ajodhia, V., Petrov, K., Scarsi, G. C., & Franken, B. (2006). Experience with Regulation of Network Quality in Italy, the UK and the Netherlands. (1), 7.

Albert, R., Albert, I., & Nakarado, G. L. (2004). Structural vulnerability of the North American power grid. *Physical Review E*, *69*(2), 025103. https://doi.org/10.1103/PhysRevE.69.025103

Albert, R., Jeong, H., & Barabási, A.-L. (2000). Error and attack tolerance of complex networks, 14.

Amaral, L. A. N., Scala, A., Barthélémy, M., & Stanley, H. E. (2000). Classes of small-world networks. *Proceedings of the National Academy of Sciences*, *97*(21), 11149–11152. https://doi.org/10.1073/pnas.200327197

Barabási, A. L., Jeong, H., Néda, Z., Ravasz, E., Schubert, A., & Vicsek, T. (2002). Evolution of the social network of scientific collaborations. *Physica A: Statistical Mechanics and its Applications*, *311*(3), 590–614. https://doi.org/10.1016/S0378-4371(02)00736-7

Barabási, A.-L., & Albert, R. (1999). Emergence of Scaling in Random Networks, 11.

Birchfield, A. B., & Overbye, T. J. (2021). Graph Crossings in Electric Transmission Grids. *2021 North American Power Symposium (NAPS)*, 1–6. https://doi.org/10.1109/NAPS52732.2021.9654543

Birchfield, A. B., Xu, T., Gegner, K. M., Shetye, K. S., & Overbye, T. J. (2017). Grid Structural Characteristics as Validation Criteria for Synthetic Networks. *IEEE Transactions on Power Systems*, *32*(4), 3258–3265. https://doi.org/10.1109/TPWRS.2016.2616385

Broder, A., Kumar, R., Maghoul, F., Raghavan, P., Rajagopalan, S., Stata, R., Tomkins, A., & Wiener, J. (2000). Graph structure in the Web. *Computer Networks*, *33*(1), 309–320. https://doi.org/10.1016/S1389-1286(00)00083-9

Broido, A. D., & Clauset, A. (2019). Scale-free networks are rare. *Nature Communications*, *10*(1), 1017. https://doi.org/10.1038/s41467-019-08746-5

Brummitt, C. D., Hines, P. D. H., Dobson, I., Moore, C., & D'Souza, R. M. (2013). Transdisciplinary electric power grid science. *Proceedings of the National Academy of Sciences*, *110*(30), 12159–12159. https://doi.org/10.1073/pnas.1309151110

Buldyrev, S. V., Parshani, R., Paul, G., Stanley, H. E., & Havlin, S. (2010). Catastrophic cascade of failures in interdependent networks. *Nature*, *464*(7291), 1025–1028. https://doi.org/10.1038/nature08932
Bandiera_abtest: a Cg_type: Nature Research Journals Primary_atype: Research Subject_term: Network models Subject_term_id: network-models

Buzna, L., Issacharoff, L., & Helbing, D. (2009). The evolution of the topology of high-voltage electricity networks. *Int. J. Crit. Infrastructures*. https://doi.org/10.1504/IJCIS.2009.022850

Carreras, B., Newman, D., & Dobson, I. (2012). Determining the Vulnerabilities of the Power Transmission System, 2044–2053. https://doi.org/10.1109/HICSS.2012.208

Carreras, B., Reynolds Barredo, J. M., Dobson, I., & Newman, D. (2019). Validating the OPA Cascading Blackout Model on a 19402 Bus Transmission Network with Both Mesh and Tree Structures. https://doi.org/10.24251/HICSS.2019.423

Chassin, D. P., Fisher, A., Fuller, J., Teyber, A., Tenney, N., Tuffner, F., Schneider, K., & Hardy, T. (2022). *HiPAS GridLAB-D* (Version 4.3.1-221128-develop_add_aws_install for Linux). Menlo Park. https://github.com/slacgismo/gridlabd

Chassin, D. P., & Posse, C. (2005). Evaluating North American electric grid reliability using the Barabási-Albert network model. *Physica A: Statistical Mechanics and its Applications*, *355*(2), 667–677. https://doi.org/10.1016/j.physa.2005.02.051

Christie, R. D. (1999). Power Systems Test Case Archive. http://labs.ece.uw.edu/pstca/

Clauset, A., Shalizi, C. R., & Newman, M. E. J. (2009). Power-Law Distributions in Empirical Data. *SIAM Review*, *51*(4), 661–703. https://doi.org/10.1137/070710111

Cloteaux, B. (2013). Limits in modeling power grid topology. *2013 IEEE 2nd Network Science Workshop (NSW)*, 16–22. https://doi.org/10.1109/NSW.2013.6609189

Cotilla-Sanchez, E., Hines, P. D. H., Barrows, C., & Blumsack, S. (2012). Comparing the Topological and Electrical Structure of the North American Electric Power Infrastructure. *IEEE Systems Journal*, *6*(4), 616–626. https://doi.org/10.1109/JSYST.2012.2183033

Crucitti, P., Latora, V., & Marchiori, M. (2004). A topological analysis of the Italian electric power grid. *Physica A: Statistical Mechanics and its Applications*, *338*(1), 92–97. https://doi.org/10.1016/j.physa.2004.02.029

Deka, D., Vishwanath, S., & Baldick, R. (2017). Analytical Models for Power Networks: The Case of the Western U.S. and ERCOT Grids. *IEEE Transactions on Smart Grid*, *8*(6), 2794–2802. https://doi.org/10.1109/TSG.2016.2540439

Erdős, P., & Rényi, A. (1959). On random graphs. I. *Publicationes Mathematicae Debrecen*, *6*(3-4), 290–297. https://doi.org/10.5486/PMD.1959.6.3-4.12

Espejo, R., Lumbreras, S., & Ramos, A. (2018). Analysis of transmission-power-grid topology and scalability, the European case study. *Physica A: Statistical Mechanics and its Applications*, *509*, 383–395. https://doi.org/10.1016/j.physa.2018.06.019

Faloutsos, M., Faloutsos, P., & Faloutsos, C. (1999). On power-law relationships of the Internet topology. *ACM SIGCOMM Computer Communication Review*, *29*(4), 251–262. https://doi.org/10.1145/316194.316229

Fox Keller, E. (2005). Revisiting "scale-free" networks. *BioEssays*, *27*(10), 1060–1068. https://doi.org/10.1002/bies.20294

Han, P., & Ding, M. (2011). Analysis of Cascading Failures in Small-world Power Grid. *International Journal of Energy Science*, *1*(2), 7.

Hartmann, B. (2021). How does the vulnerability of an evolving power grid change? *Electric Power Systems Research*, *200*, 107478. https://doi.org/10.1016/j.epsr.2021.107478

Hartmann, B., & Sugár, V. (2021). Searching for small-world and scale-free behaviour in long-term historical data of a real-world power grid. *Scientific Reports*, *11*(1), 6575. https://doi.org/10.1038/s41598-021-86103-7

Holme, P. (2019). Rare and everywhere: Perspectives on scale-free networks. *Nature Communications*, *10*(1), 1016. https://doi.org/10.1038/s41467-019-09038-8

Holmgren, Å. J. (2006). Using Graph Models to Analyze the Vulnerability of Electric Power Networks. *Risk Analysis*, *26*(4), 955–969. https://doi.org/10.1111/j.1539-6924.2006.00791.x

Hutcheon, N., & Bialek, J. W. (2013). Updated and validated power flow model of the main continental European transmission network. *2013 IEEE Grenoble Conference*, 1–5. https://doi.org/10.1109/PTC.2013.6652178

Jeong, H., Néda, Z., & Barabási, A. L. (2003). Measuring preferential attachment in evolving networks. *Europhysics Letters (EPL)*, *61*(4), 567–572. https://doi.org/10.1209/epl/i2003-00166-9

Kim, H., Olave-Rojas, D., Álvarez-Miranda, E., & Son, S.-W. (2018). In-depth data on the network structure and hourly activity of the Central Chilean power grid. *Scientific Data*, *5*(1), 180209. https://doi.org/10.1038/sdata.2018.209

Klein, D. J., & Randić, M. (1993). Resistance distance. *Journal of Mathematical Chemistry*, *12*(1), 81–95. https://doi.org/10.1007/BF01164627

Kruiskamp, P. (2022). *Standaard Bedrijfs Indeling 2008. Versie 2018, Update 2022*. Centraal Bureau voor de Statistiek. https://www.cbs.nl/nl-nl/onze-diensten/methoden/classificaties/activiteiten/sbi-2008-standaard-bedrijfsindeling-2008/de-structuur-van-de-sbi-2008-versie-2018-update-2022

Latora, V., & Marchiori, M. (2007). A measure of centrality based on network efficiency. *New Journal of Physics*, *9*(6), 188–188. https://doi.org/10.1088/1367-2630/9/6/188

Latora, V., & Marchiori, M. (2001). Efficient Behavior of Small-World Networks. *Physical Review Letters*, *87*(19), 198701. https://doi.org/10.1103/PhysRevLett.87.198701

Leuthold, F. U., Weigt, H., & von Hirschhausen, C. (2012). A Large-Scale Spatial Optimization Model of the European Electricity Market. *Networks and Spatial Economics*, *12*(1), 75–107. https://doi.org/10.1007/s11067-010-9148-1

Matke, Carsten, Medjroubi, W., & Kleinhans, D. (2016). SciGRID - An Open Source Reference Model for the European Transmission Network (v0.2). http://www.scigrid.de

Mei, S., Zhang, X., & Cao, M. (2011). Power Grid Growth and Evolution. In S. Mei, X. Zhang, & M. Cao (Eds.), *Power Grid Complexity* (pp. 133–160). Springer. https://doi.org/10.1007/978-3-642-16211-4_4

Menck, P. J., Heitzig, J., Kurths, J., & Joachim Schellnhuber, H. (2014). How dead ends undermine power grid stability. *Nature Communications*, *5*(1), 3969. https://doi.org/10.1038/ncomms4969

Nesti, T., Zocca, A., & Zwart, B. (2018). Emergent failures and cascades in power grids: A statistical physics perspective, 18.

Newman, M. E. J. (2001). Clustering and preferential attachment in growing networks. *Physical Review E*, *64*(2), 025102. https://doi.org/10.1103/PhysRevE.64.025102

Pagani, G. A., & Aiello, M. (2011). Towards Decentralization: A Topological Investigation of the Medium and Low Voltage Grids. *IEEE Transactions on Smart Grid*, *2*(3), 538–547. https://doi.org/10.1109/TSG.2011.2147810

Pham, T., Sheridan, P., & Shimodaira, H. (2015). PAFit: A Statistical Method for Measuring Preferential Attachment in Temporal Complex Networks. *PLOS ONE*, *10*(9), e0137796. https://doi.org/10.1371/journal.pone.0137796

Price, D. J. d. S. (1965). Networks of Scientific Papers. *Science*, *149*(3683), 510–515. https://doi.org/10.1126/science.149.3683.510

Rosas-Casals, M., Valverde, S., & Solé, R. V. (2007). Topological vulnerability of the European power grid under errors and attacks. *International Journal of Bifurcation and Chaos*, *17*(07), 2465–2475. https://doi.org/10.1142/S0218127407018531

Rosato, V., Bologna, S., & Tiriticco, F. (2007). Topological properties of high-voltage electrical transmission networks. *Electric Power Systems Research*, *77*(2), 99–105. https://doi.org/10.1016/j.epsr.2005.05.013

Schweitzer, E., Scaglione, A., Monti, A., & Pagani, G. A. (2017). Automated Generation Algorithm for Synthetic Medium Voltage Radial Distribution Systems. *IEEE Journal on Emerging and Selected Topics in Circuits and Systems*, *7*(2), 271–284. https://doi.org/10.1109/JETCAS.2017.2682934

Simonsen, I., Buzna, L., Peters, K., Bornholdt, S., & Helbing, D. (2008). Transient Dynamics Increasing Network Vulnerability to Cascading Failures. *Physical Review Letters*, *100*(21), 218701. https://doi.org/10.1103/PhysRevLett.100.218701

Snodgrass, J., Kunkolienkar, S., Habiba, U., Liu, Y., Stevens, M., Safdarian, F., Overbye, T., & Korab, R. (2022). Case Study of Enhancing the MATPOWER Polish Electric Grid. *2022 IEEE Texas Power and Energy Conference (TPEC)*, 1–6. https://doi.org/10.1109/TPEC54980.2022.9750807

TenneT. (2022c). Hoogspanningsnet Nederland - Asset gegevens. https://www.arcgis.com/home/item.html?id=a78be8a36dd544afab94c996d1475632

TenneT. (2023). *Overzicht van de 380kV en 220kV componenten*. https://netztransparenz.tennet.eu/nl/elektriciteitsmarkt/transparantiepaginas/overzicht-van-de-380kv-en-220kv-componenten/

Wang, Z., Scaglione, A., & Thomas, R. J. (2010). Generating Statistically Correct Random Topologies for Testing Smart Grid Communication and Control Networks. *IEEE Transactions on Smart Grid*, *1*(1), 28–39. https://doi.org/10.1109/TSG.2010.2044814

Watts, D. J., & Strogatz, S. H. (1998). Collective dynamics of 'small-world' networks. *393*, 3.

Wiegmans, B. (2016a). GridKit: European and North-American extracts. https://doi.org/10.5281/zenodo.47317

Wiegmans, B. (2016b). GridKit extract of ENTSO-E interactive map. https://doi.org/10.5281/zenodo.55853

Zimmerman, R. D., Murillo-Sanchez, C. E., & Thomas, R. J. (2011). MATPOWER: Steady-State Operations, Planning, and Analysis Tools for Power Systems Research and Education. *IEEE Transactions on Power Systems*, *26*(1), 12–19. https://doi.org/10.1109/TPWRS.2010.2051168

Chapter 8

Bibliography – maps

Arnhemse Instellingen van de Elektriciteitsbedrijven. (1971). *Elektriciteit in Nederland 1970*.

Arnhemse Instellingen van de Elektriciteitsbedrijven. (1972). *Elektriciteit in Nederland 1971*.

Centraal Bureau voor de Statistiek. (1933a). *Electriciteitsstatistiek 1930*. Vereeniging van Directeuren van Electriciteitsbedrijven in Nederland.

Centraal Bureau voor de Statistiek. (1933b). *Electriciteitsstatistiek 1931*.

Centraal Bureau voor de Statistiek. (1934). *Electriciteitsstatistiek 1932*.

Centraal Bureau voor de Statistiek. (1935). *Electriciteitsstatistiek 1933*.

Centraal Bureau voor de Statistiek. (1936). *Electriciteitsstatistiek 1934*.

Centraal Bureau voor de Statistiek. (1937). *Electriciteitsstatistiek 1935*.

Centraal Bureau voor de Statistiek. (1938). *Electriciteitsstatistiek 1936*.

Centraal Bureau voor de Statistiek. (1939). *Electriciteitsstatistiek 1937*.

Centraal Bureau voor de Statistiek. (1941a). *Electriciteitsstatistiek 1938*.

Centraal Bureau voor de Statistiek. (1941b). *Electriciteitsstatistiek 1939*.

Directie Arnhemse instellingen van de elektriciteitsbedrijven. (1974). *Elektriciteit in Nederland 1973*.

Directie Arnhemse instellingen van de elektriciteitsbedrijven. (1975). *Elektriciteit in Nederland 1974*.

Directie Arnhemse instellingen van de elektriciteitsbedrijven. (1976). *Elektriciteit in Nederland 1975*.

Directie Arnhemse instellingen van de elektriciteitsbedrijven. (1977). *Elektriciteit in Nederland 1976*.

Directie Arnhemse instellingen van de elektriciteitsbedrijven. (1978). *Elektriciteit in Nederland 1977*.

Directie Arnhemse instellingen van de elektriciteitsbedrijven. (1979). *Elektriciteit in Nederland 1978*.

Directie Arnhemse instellingen van de elektriciteitsbedrijven. (1980). *Elektriciteit in Nederland 1979*.

Directie Arnhemse instellingen van de elektriciteitsbedrijven in Nederland. (1981). *Elektriciteit in Nederland 1980*.

Directie Arnhemse instellingen van de elektriciteitsbedrijven in Nederland. (1982). *Elektriciteit in Nederland 1981*.

Directie Arnhemse instellingen van de elektriciteitsbedrijven in Nederland. (1983). *Elektriciteit in Nederland 1982*.

Directie Arnhemse instellingen van de elektriciteitsbedrijven in Nederland. (1984). *Elektriciteit in Nederland 1983*.

Directies Arnhemse instellingen van de elektriciteitsbedrijven in Nederland. (1985). *Elektriciteit in Nederland 1984*.

Empelen, v., Louis. (N.d.). *'De Grootsche Gedachte van het Koppelen der Centrales'. De aanleg van het hoogspanningskoppelnet in Zuid-Holland in de periode 1930-1945*. https://pv-eon-benelux.nl/Historie/1%20Transport/Transport%20documenten/EZH%20boek.pdf

N.V. Samenwerkende Electriciteits-Productiebedrijven. (1950). *Verslag over het jaar 1949*. N.V. Samenwerkende Electriciteits-Productiebedrijven. Arnhem.

N.V. Samenwerkende Electriciteits-Productiebedrijven. (1951). *Verslag over het jaar 1950*. N.V. Samenwerkende Electriciteits-Productiebedrijven. Arnhem.

N.V. Samenwerkende Electriciteits-Productiebedrijven. (1952). *Verslag over het jaar 1951*. N.V. Samenwerkende Electriciteits-Productiebedrijven. Arnhem.

N.V. Samenwerkende Electriciteits-Productiebedrijven. (1953). *Verslag over het jaar 1952*. N.V. Samenwerkende Electriciteits-Productiebedrijven. Arnhem.

N.V. Samenwerkende Electriciteits-Productiebedrijven. (1956). *Verslag over het jaar 1955*. N.V. Samenwerkende Electriciteits-Productiebedrijven. Arnhem.

N.V. Samenwerkende Electriciteits-Productiebedrijven. (1957). *Verslag over het jaar 1956*. N.V. Samenwerkende Electriciteits-Productiebedrijven. Arnhem.

N.V. Samenwerkende Electriciteits-Productiebedrijven. (1958). *Verslag over het jaar 1957*. N.V. Samenwerkende Electriciteits-Productiebedrijven. Arnhem.

N.V. Samenwerkende Electriciteits-Productiebedrijven. (1959). *Verslag over het jaar 1958*. N.V. Samenwerkende Electriciteits-Productiebedrijven. Arnhem.

N.V. Samenwerkende Electriciteits-Productiebedrijven. (1960). *Verslag over het jaar 1959*. N.V. Samenwerkende Electriciteits-Productiebedrijven. Arnhem.

N.V. Samenwerkende Electriciteits-Productiebedrijven. (1961). *Verslag over het jaar 1960*. N.V. Samenwerkende Electriciteits-Productiebedrijven. Arnhem.

N.V. Samenwerkende Electriciteits-Productiebedrijven. (1962). *Verslag over het jaar 1961*. N.V. Samenwerkende Electriciteits-Productiebedrijven. Arnhem.

N.V. Samenwerkende Electriciteits-Productiebedrijven. (1963). *Verslag over het jaar 1962*. N.V. Samenwerkende Electriciteits-Productiebedrijven. Arnhem.

N.V. Samenwerkende Electriciteits-Productiebedrijven. (1964). *Verslag over het jaar 1963*. N.V. Samenwerkende Electriciteits-Productiebedrijven. Arnhem.

N.V. Samenwerkende Electriciteits-Productiebedrijven. (1965). *Verslag over het jaar 1964*. N.V. Samenwerkende Electriciteits-Productiebedrijven. Arnhem.
N.V. Samenwerkende Electriciteits-Productiebedrijven. (1966). *Verslag over het jaar 1965*. N.V. Samenwerkende Electriciteits-Productiebedrijven. Arnhem.
N.V. Samenwerkende Electriciteits-Productiebedrijven. (1967). *Verslag over het jaar 1966*. N.V. Samenwerkende Elektriciteits-Produktiebedrijven. Arnhem.
N.V. Samenwerkende Electriciteits-Productiebedrijven. (1968). *Verslag over het jaar 1967*. N.V. Samenwerkende Electriciteits-Productiebedrijven. Arnhem.
N.V. Samenwerkende Electriciteits-Productiebedrijven. (1969). *Verslag over het jaar 1968*. N.V. Samenwerkende Electriciteits-Productiebedrijven. Arnhem.
N.V. Samenwerkende Electriciteits-Productiebedrijven. (1970). *Verslag over het jaar 1969*. N.V. Samenwerkende Electriciteits-Productiebedrijven. Arnhem.
N.V. Samenwerkende Electriciteits-Productiebedrijven. (1971). *Verslag over het jaar 1970*. N.V. Samenwerkende Electriciteits-Productiebedrijven. Arnhem.
N.V. Samenwerkende Elektriciteits-Produktiebedrijven. (1972). *Verslag over het jaar 1971*. N.V. Samenwerkende Elektriciteits-Produktiebedrijven. Arnhem.
N.V. Samenwerkende Elektriciteits-Produktiebedrijven. (1973). *Verslag over het jaar 1972*. N.V. Samenwerkende Elektriciteits-Produktiebedrijven. Arnhem.
N.V. Samenwerkende Elektriciteits-Produktiebedrijven. (1974). *Verslag over het jaar 1973*. N.V. Samenwerkende Elektriciteits-Produktiebedrijven. Arnhem.
N.V. Samenwerkende Elektriciteits-Produktiebedrijven. (1975). *Verslag over het jaar 1974*. N.V. Samenwerkende Elektriciteits-Produktiebedrijven. Arnhem.
N.V. Samenwerkende Elektriciteits-Produktiebedrijven. (1976). *Verslag over het jaar 1975*. N.V. Samenwerkende Elektriciteits-Produktiebedrijven. Arnhem.
N.V. Samenwerkende Elektriciteits-Produktiebedrijven. (1977). *Verslag over het jaar 1976*. N.V. Samenwerkende Elektriciteits-Produktiebedrijven. Arnhem.
N.V. Samenwerkende Elektriciteits-Produktiebedrijven. (1978). *Verslag over het jaar 1977*. N.V. Samenwerkende Elektriciteits-Produktiebedrijven. Arnhem.
N.V. Samenwerkende Elektriciteits-Produktiebedrijven. (1979). *Verslag over het jaar 1978*. N.V. Samenwerkende Elektriciteits-Produktiebedrijven. Arnhem.
N.V. Samenwerkende Elektriciteits-Produktiebedrijven. (1980). *Verslag over het jaar 1979*. N.V. Samenwerkende Elektriciteits-Produktiebedrijven. Arnhem.
N.V. Samenwerkende Elektriciteits-Produktiebedrijven. (1981). *Verslag over het jaar 1980*. N.V. Samenwerkende Elektriciteits-Produktiebedrijven. Arnhem.
N.V. Samenwerkende Elektriciteits-Produktiebedrijven. (1982). *Verslag over het jaar 1981*. N.V. Samenwerkende Elektriciteits-Produktiebedrijven. Arnhem.
N.V. Samenwerkende Elektriciteits-Produktiebedrijven. (1983). *Verslag over het jaar 1982*. N.V. Samenwerkende Elektriciteits-Produktiebedrijven. Arnhem.
N.V. Samenwerkende Elektriciteits-Produktiebedrijven. (1984). *Verslag over het jaar 1983*. N.V. Samenwerkende Elektriciteits-Produktiebedrijven. Arnhem.
N.V. Samenwerkende Elektriciteits-Produktiebedrijven. (1985). *Verslag over het jaar 1984*. N.V. Samenwerkende Elektriciteits-Produktiebedrijven. Arnhem.
N.V. Samenwerkende Elektriciteits-Produktiebedrijven. (1986). *Verslag over het jaar 1985*. N.V. Samenwerkende Elektriciteits-Produktiebedrijven. Arnhem.
N.V. Samenwerkende Elektriciteits-Produktiebedrijven. (1987). *Verslag over het jaar 1986*. N.V. Samenwerkende Elektriciteits-Produktiebedrijven. Arnhem.
N.V. Samenwerkende Elektriciteits-Produktiebedrijven. (1988). *Verslag over het jaar 1987*. N.V. Samenwerkende Elektriciteits-Produktiebedrijven. Arnhem.
N.V. Samenwerkende Elektriciteits-Produktiebedrijven. (1989). *Verslag over het jaar 1988*. N.V. Samenwerkende Elektriciteits-Produktiebedrijven. Arnhem.
N.V. Samenwerkende Elektriciteits-Produktiebedrijven. (1990). *Verslag over het jaar 1989*. N.V. Samenwerkende Elektriciteits-Produktiebedrijven. Arnhem.
N.V. Samenwerkende Elektriciteits-Produktiebedrijven. (1993). *Verslag over het jaar 1992*. N.V. Samenwerkende Elektriciteits-Produktiebedrijven. Arnhem.
N.V. Samenwerkende Elektriciteits-Produktiebedrijven. (1994). *Verslag over het jaar 1993*. N.V. Samenwerkende Elektriciteits-Produktiebedrijven. Arnhem.
N.V. Samenwerkende Elektriciteits-Produktiebedrijven. (1995). *Verslag over het jaar 1994*. N.V. Samenwerkende Elektriciteits-Produktiebedrijven. Arnhem.
N.V. Samenwerkende Elektriciteits-Produktiebedrijven. (1996). *Verslag over het jaar 1995*. N.V. Samenwerkende Elektriciteits-Produktiebedrijven. Arnhem.
N.V. Samenwerkende Elektriciteits-Produktiebedrijven. (1997). *Verslag over het jaar 1996*. N.V. Samenwerkende Elektriciteits-Produktiebedrijven. Arnhem.
N.V. Samenwerkende Elektriciteits-Produktiebedrijven. (1998). *Verslag over het jaar 1997*. N.V. Samenwerkende Elektriciteits-Produktiebedrijven. Arnhem.
N.V. Samenwerkende Elektriciteits-Produktiebedrijven, N.V. Gemeenschappelijke Kernenergiecentrale Nederland, N.V. tot Keuring van Elektrotechnische Materialen, Vereniging van Exploitanten van Electriciteitsbedrijven in Nederland, & Vereniging van Directeuren van Elektriciteitsbedrijven in Nederland. (1973). *Elektriciteit in Nederland 1972*.
N.V. Samenwerkende Elektriciteits-Produktiebedrijven, N.V. Gemeenschappelijke Kernenergiecentrale Nederland, N.V. tot Keuring van Elektrotechnische Materialen, Vereniging van Exploitanten van Elektriciteitsbedrijven in Nederland, & Vereniging van Directeuren van Elektriciteitsbedrijven in Nederland. (1986). *Elektriciteit in Nederland 1985*.
N.V. Samenwerkende Elektriciteits-Produktiebedrijven, N.V. Gemeenschappelijke Kernenergiecentrale Nederland, N.V. tot Keuring van Elektrotechnische Materialen, Vereniging van Exploitanten van Elektriciteitsbedrijven in Nederland, & Vereniging van Directeuren van Elektriciteitsbedrijven in Nederland. (1987). *Elektriciteit in Nederland 1986*.

N.V. Samenwerkende Elektriciteits-Produktiebedrijven, N.V. Gemeenschappelijke Kernenergiecentrale Nederland, N.V. tot Keuring van Elektrotechnische Materialen, Vereniging van Exploitanten van Elektriciteitsbedrijven in Nederland, & Vereniging van Directeuren van Elektriciteitsbedrijven in Nederland. (1988). *Elektriciteit in Nederland 1987*.
N.V. Samenwerkende Elektriciteits-Produktiebedrijven & Vereniging van Energiedistributiebedrijven in Nederland. (1993). *Elektriciteit in Nederland 1992*.
N.V. Samenwerkende Elektriciteits-Produktiebedrijven & Vereniging van Energiedistributiebedrijven in Nederland. (1994). *Elektriciteit in Nederland 1993*.
N.V. Samenwerkende Elektriciteits-Produktiebedrijven & Vereniging van Energiedistributiebedrijven in Nederland. (1995). *Elektriciteit in Nederland 1994*.
N.V. Samenwerkende Elektriciteits-Produktiebedrijven & Vereniging van Energiedistributiebedrijven in Nederland. (1996). *Elektriciteit in Nederland 1995*.
N.V. Samenwerkende Elektriciteits-Produktiebedrijven & Vereniging van Exploitanten van Elektriciteitsbedrijven in Nederland. (1990). *Elektriciteit in Nederland 1989*.
N.V. Samenwerkende Elektriciteits-Produktiebedrijven & Vereniging van Exploitanten van Elektriciteitsbedrijven in Nederland. (1991). *Elektriciteit in Nederland 1990*.
N.V. Samenwerkende Elektriciteits-Produktiebedrijven & Vereniging van Exploitanten van Elektriciteitsbedrijven in Nederland. (1992). *Elektriciteit in Nederland 1991*.
N.V. Samenwerkende Elektriciteits-Produktiebedrijven, Vereniging van Exploitanten van Elektriciteitsbedrijven in Nederland, & N.V. tot Keuring van Elektrotechnische Materialen. (1989). *Elektriciteit in Nederland 1988*.
TenneT. (2001). *Jaarverslag 2000*. TenneT. Arnhem. https://web.archive.org/web/20030429201426/http://www.tennet.org/images/14_1602.pdf
TenneT. (2002a). Nederlands hoogspanningsnet. https://web.archive.org/web/20030903034549/http://www.tennet.org:80/images/14_1863.pdf
TenneT. (2002b). *Jaarverslag 2001*. https://web.archive.org/web/20071213155646/http://www.tennet.org/images/2001%20JV%20NL%20Totaal_tcm41-11555.pdf
TenneT. (2003). *Jaarverslag 2002*. https://web.archive.org/web/20071213155916/http://www.tennet.org/images/2002%20JV%20NL%20Totaal_tcm41-11554.pdf
TenneT. (2004a). Nederlands hoogspanningsnet. https://web.archive.org/web/20061007134637/http://www.tennet.nl/images/netkaart2004_tcm41-12264.pdf
TenneT. (2004b). *Jaarverslag 2003*. https://web.archive.org/web/20071213155236/http://www.tennet.org/images/2003%20JV%20NL%20Totaal_tcm41-11553.pdf
TenneT. (2005). *Jaarverslag 2004*. https://web.archive.org/web/20071213160116/http://www.tennet.org/images/2004%20JV%20NL%20Totaal_tcm41-11552.pdf
TenneT. (2006). *Jaarverslag 2005*. https://web.archive.org/web/20071213112734/http://www.tennet.org/images/Deel%201_tcm41-12948.pdf
TenneT. (2007a). *Jaarverslag 2006*. https://web.archive.org/web/20071214105305/http://www.tennet.org/images/TenneT_jaarverslag_2006_deel1_tcm41-13756.pdf
TenneT. (2007b). Nederlands transportnet. https://web.archive.org/web/20070927062528/http://www.tennet.nl/images/Netkaart%202007_tcm41-13639.pdf
TenneT. (2008). Elektriciteitstransportnet TenneT TSO B.V.
TenneT. (2009). *Jaarverslag 2008*. https://www.tennet.eu/fileadmin/user_upload/Company/Investor_Relations/Annual_Report/TenneT-AR08_nl.pdf
TenneT. (2010). *Jaarverslag 2009*. https://www.tennet.eu/fileadmin/user_upload/Company/Investor_Relations/Annual_Report/TenneT-AR09.pdf
TenneT. (2011a). *Jaarverslag 2010*. https://www.tennet.eu/fileadmin/user_upload/Company/Investor_Relations/Annual_Report/TenneT-AR10.pdf
TenneT. (2011b). Nederlands transportnet.
TenneT. (2012). *Jaarverslag 2011*. https://www.tennet.eu/fileadmin/user_upload/Company/Investor_Relations/Annual_Report/TenneT-AR11.pdf
TenneT. (2013). *Integrated Annual Report TenneT 2012*. https://www.tennet.eu/fileadmin/user_upload/Company/Investor_Relations/Annual_Report/Integrated_Annual_Report_2012.pdf
TenneT. (2014). *Integrated Annual Report TenneT 2013*. https://www.tennet.eu/fileadmin/user_upload/Company/Investor_Relations/Annual_Report/TenneT-AR13_UK.pdf
TenneT. (2015). *Integrated Annual Report 2014 TenneT Holding B.V.* https://www.tennet.eu/fileadmin/user_upload/Company/Investor_Relations/Annual_Report/TenneT-AR14_UK.pdf
TenneT. (2016a). *Integrated Annual Report 2015 TenneT Holding B.V.* https://www.tennet.eu/fileadmin/user_upload/Company/Investor_Relations/Annual_Report/TenneT-AR15_UK.pdf
TenneT. (2016b). Netkaart TenneT (Nederland en Duitsland). https://web.archive.org/web/20170223232822/http://www.tennet.eu/fileadmin/user_upload/Company/Publications/Gridmaps/16_08_2016DE_G058_16-140_GridMap-technisch_V2.pdf
TenneT. (2017a). Netkaart Nederland. https://web.archive.org/web/20170315174316if_/http://www.tennet.eu/fileadmin/user_upload/Company/Publications/Gridmaps/NL/Gridmap_Netherlands_NL.pdf
TenneT. (2017b). Nederlands transportnet 2017. https://www.hoogspanningsnet.com/wp-content/uploads/TenneT-netkaart_extern-2017.jpg
TenneT. (2018). Netkaart (technical overview). https://web.archive.org/web/20210624085738/https://www.tennet.eu/fileadmin/user_upload/Company/Publications/Gridmaps/DE/G019_18-120_GridMap_V2-D-NL-e.pdf
TenneT. (2019). Netkaart Nederland. https://www.tennet.eu/fileadmin/user_upload/Company/Publications/Gridmaps/NL/Gridmap_Netherlands_NL_2019.pdf
TenneT. (2020a). Nederlands transportnet 2020. https://www.hoogspanningsnet.com/wp-content/uploads/Tennet-Netkaart-2020-scaled.jpg
TenneT. (2020b). Netkaart Nederland. https://www.tennet.eu/fileadmin/user_upload/Company/Publications/Gridmaps/NL/0403-189_NETHERLANDS_nl_dl_100pct_V15.pdf

TenneT. (2020c). Netkaart Nederland. https://web.archive.org/web/20210928120023/https://www.tennet.eu/fileadmin/user_upload/Company/Publications/Gridmaps/NL/NETHERLANDS_nl_sl_33pct_V16_200630_HiRes.pdf
TenneT. (2020d). Netkaart Nederland Offshore. https://web.archive.org/web/20210228152931/https://www.tennet.eu/fileadmin/user_upload/Company/Publications/Gridmaps/NL/NETHERLANDS_OFFSHORE_nl_el_100pct_V16_200630_HiRes.pdf
TenneT. (2020e). Netkaart TenneT. https://web.archive.org/web/20210929035714/https://www.tennet.eu/fileadmin/user_upload/Company/Publications/Gridmaps/NL/TENNET_nl_sl_33pct_V16_200630_HiRes.pdf
TenneT. (2021). Netkaart TenneT. https://web.archive.org/web/20210515141336/https://www.tennet.eu/fileadmin/user_upload/Company/Publications/Gridmaps/DE/G019_21-010_GridMap_V9-D-NL-d.pdf
TenneT. (2022a). Netkaart Offshore Nederland. https://www.tennet.eu/fileadmin/user_upload/Company/Publications/Gridmaps/NL/2021_1/NL_DEC2021_Offshore_Netherlands_01.pdf
TenneT. (2022b). Netkaart Onshore Nederland. https://www.tennet.eu/fileadmin/user_upload/Company/Publications/Gridmaps/NL/2021_1/NL_DEC2021_Onshore_Netherlands_01.pdf
Vereeniging van Directeuren van Electriciteitsbedrijven in Nederland. (1926). *De ontwikkeling van de electriciteitsvoorziening van Nederland tot het jaar 1925*. Van Kampen. https://resolver.kb.nl/resolve?urn=MMKB02:000122393:00649
Vereeniging van Directeuren van Electriciteitsbedrijven in Nederland. (1948). *De ontwikkeling van onze electriciteitsvoorziening 1880-1938. Deel II*. Centraal Bureau.

Appendix A

Power flow parameters

A.1 Determining electrical parameters

To calculate the power flows, at a minimum the following electrical parameters need to be known:

- Impedance (resistance and reactance) of every transmission line
- Capacity of every transmission lines
- Transforming capacities of every transformer

For current transmission lines at 220kV and 380kV, the impedances parameters are documented (TenneT, 2023). For lower voltages and previously existing lines, we need to come up with an estimate. We can decompose the impedance of a line as the specific impedance (per length unit) times the length of the line. In order to get a good estimate of the specific impedances, we plot the known impedances over time in Figures A.1 and A.2. We also need a good length estimate per line. Since we don't know the exact line trajectory, and thus also not the exact line length, we have to estimate this using the coordinates of the endpoints of the lines. See Figure A.3.

Figure A.1: Plot of the specific resistance of transmission lines against the (estimated) build year of the line. Based on data from TenneT (2023).

Figure A.2: Plot of the specific reactance of transmission lines against the (estimated) build year of the line. Based on data from TenneT (2023).

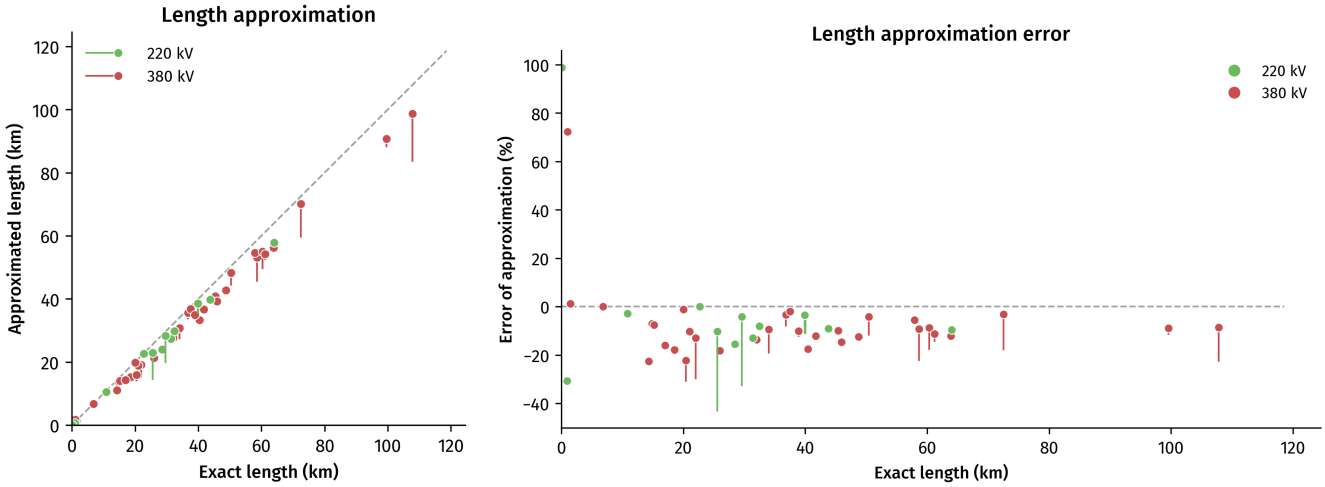

Figure A.3: Estimated line length versus the documented line length. For longer lines, the errors are relatively small (within 20%) of real values, especially when we take into account the intermediate junctions and taps of a line circuit.

A.2 Estimating load curves per substation

A difficult part in calculating the power flow is determining the load per substation at any given moment. For the Netherlands, we have the following data for recent years:

- Hourly generation per power plant, hourly cross-border flows and hourly total load going (from ENTSOE-E).
- Information per substation on the nature of the load: no load (pure transmission substations), or a mix of residential, commercial and industrial load.
- Per neighborhood ('buurt'): population, the number of households and dwellings, and the average electricity consumption; and the number of companies, divided per sector (various industrial and commercial categories) (CBS 'Wijk- en Buurtkaart')
- Yearly energy balance, including electricity use per sector (CBS).

We combine this as follows to get an average load per substation: we assign neighborhoods to their closest substation, as seen in Figure A.4. From the CBS data, we have the yearly electricity consumption per neighborhood, so the sum of these neighborhoods forms the residential component of the substations loads.

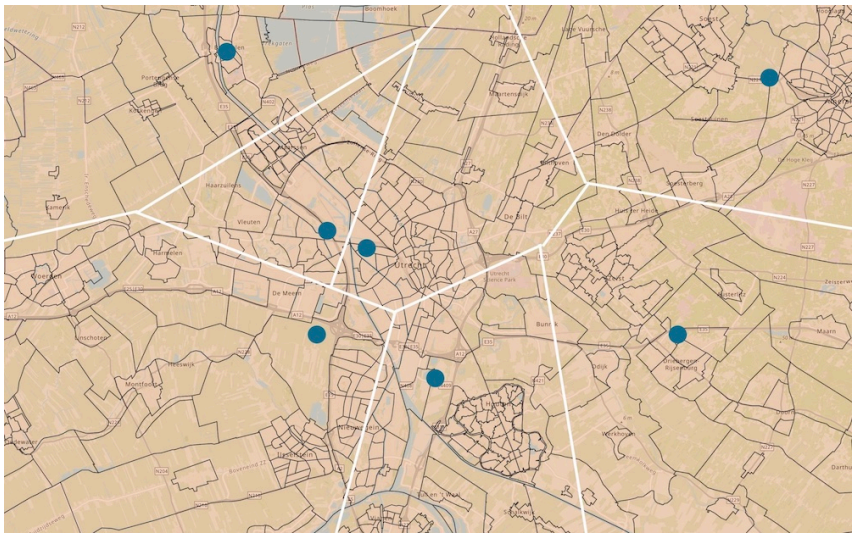

Figure A.4: An example of the method to assign neighborhoods to substations, for the Dutch city of Utrecht. The black lines are the borders of the statistical 'buurt' (neighborhood) units as defined by the CBS. The blue circles are the locations of the substations that are connected to the distribution system. The white lines are the borders of the area served by a specific substation. We assume the distribution systems of neighborhoods are connected to the closest transmission substation, so this creates a Voronoi diagram.

The total yearly industrial and commercial load can be derived from the energy balance. We use the business sector information from the CBS to divide business types into industrial and commercial loads (Kruiskamp, 2022): the industrial is sectors A to F, and the commercial category is G to U. Furthermore, we know the number of industrial and commercial business locations per neighborhood. Since the amount of energy consumed per location is not uniform – especially for industrial loads – we assign 50% of the industrial load and 95% of the commercial load according to the number of locations in a neighborhood. The remaining 50% and 5% of the load we spread out uniformly over those substations for which we know that they *only* serve industrial or commercial loads, respectively. For industrial loads, these substations are usually located in an industrial area, or near green houses. For commercial loads, these are substations directly connected to a large data center.

If we then sum the industrial, commercial, and residential loads, we get a load per substation. The distribution of these loads – for loads with at least some load – is given in Figure A.5.

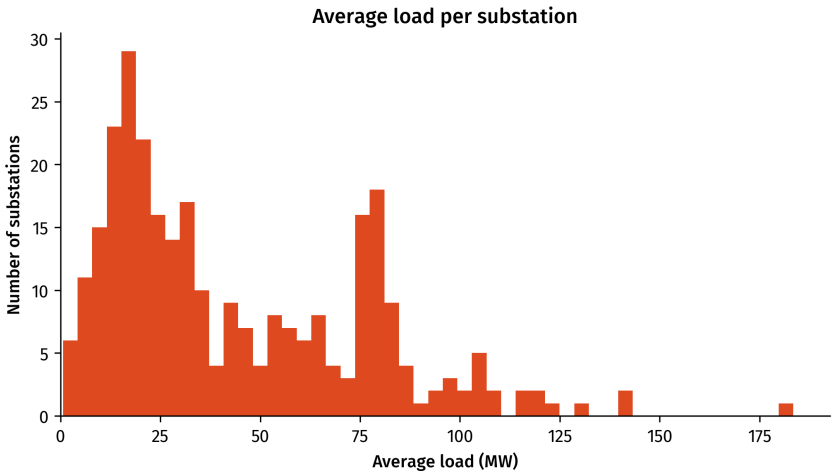

Figure A.5: Distribution of loads per substations. Substations without a load (purely transforming substations) are not included.

Appendix B

Historical maps of the Dutch grid

Source	Date (depiction)	Reference
De ontwikkeling van de electriciteitsvoorziening van Nederland tot het jaar 1925	1924-12-31	Vereeniging van Directeuren van Electriciteitsbedrijven in Nederland (VDEN, 1926)
Electriciteitsstatistiek 1930	1931-01-01	CBS (1933a)
Electriciteitsstatistiek 1931	1932-01-01	CBS (1933b)
Electriciteitsstatistiek 1932	1933-01-01	CBS (1934)
Electriciteitsstatistiek 1933	1934-01-01	CBS (1935)
Electriciteitsstatistiek 1934	1935-01-01	CBS (1936)
Electriciteitsstatistiek 1935	1936-01-01	CBS (1937)
Electriciteitsstatistiek 1936	1937-01-01	CBS (1938)
De Ontwikkeling van Onze Electriciteitsvoorziening 1880-1938. Deel II	1938	VDEN (1948)
Electriciteitsstatistiek 1937	1938-01-01	CBS (1939)
Electriciteitsstatistiek 1938	1939-01-01	CBS (1941a)
Electriciteitsstatistiek 1939	1940-01-01	CBS (1941b)
'De Grootsche Gedachte van Het Koppelen Der Centrales'. De Aanleg van Het Hoogspannings-Koppelnet in Zuid-Holland in de Periode 1930-1945	1946-1-1	Empelen (n.d.)
Verslag over Het Jaar 1949	1949, end	SEP (1950)
Verslag over Het Jaar 1950	1950, end	SEP (1951)
Verslag over Het Jaar 1951	1951, end	SEP (1952)
Verslag over Het Jaar 1952	1952, end	SEP (1953)
Verslag over Het Jaar 1955	1955-07-1	SEP (1956)
Verslag over Het Jaar 1956	1956, end	SEP (1957)
Verslag over Het Jaar 1957	1957, end	SEP (1958)
Verslag over Het Jaar 1958	1958, end	SEP (1959)
Verslag over Het Jaar 1959	1959, end	SEP (1960)
Verslag over Het Jaar 1960	1960, end	SEP (1961)
Verslag over Het Jaar 1961	1961, end	SEP (1962)
Verslag over Het Jaar 1962	1962	SEP (1963)
Verslag over Het Jaar 1963	1963	SEP (1964)
Verslag over Het Jaar 1964	1964	SEP (1965)
Verslag over Het Jaar 1965	1965-12-31	SEP (1966)
Verslag over Het Jaar 1966	1966-12-31	SEP (1967)

Verslag over Het Jaar 1967	1967	SEP (1968)
Verslag over Het Jaar 1968	1968-12-31	SEP (1969)
Verslag over Het Jaar 1969	1969	SEP (1970)
Elektriciteit in Nederland 1970	1970	Arnhemse Instellingen van de Elektriciteitsbedrijven (AIe, 1971)
Verslag over Het Jaar 1970	1970-12-31	SEP (1971)
Elektriciteit in Nederland 1971	1971, end	AIe (1972)
Verslag over Het Jaar 1971	1971-12-31	SEP (1972)
Elektriciteit in Nederland 1972	1972, end	N.V. Samenwerkende Elektriciteits-Produktiebedrijven et al. (SEP/GKN/KEMA/VEEN/VDEN, 1973)
Verslag over Het Jaar 1972	1972-12-31	SEP (1973)
Elektriciteit in Nederland 1973	1973, end	Directie Arnhemse instellingen van de elektriciteitsbedrijven (AIe, 1974)
Verslag over Het Jaar 1973	1973-12-31	SEP (1974)
Elektriciteit in Nederland 1974	1974, end	AIe (1975)
Verslag over Het Jaar 1974	1974-12-31	SEP (1975)
Elektriciteit in Nederland 1975	1975, end	AIe (1976)
Verslag over Het Jaar 1975	1975, end	SEP (1976)
Elektriciteit in Nederland 1976	1976, end	AIe (1977)
Verslag over Het Jaar 1976	1976, end	SEP (1977)
Elektriciteit in Nederland 1977	1977, end	AIe (1978)
Verslag over Het Jaar 1977	1977, end	SEP (1978)
Elektriciteit in Nederland 1978	1978, end	AIe (1979)
Verslag over Het Jaar 1978	1978, end	SEP (1979)
Elektriciteit in Nederland 1979	1979, end	AIe (1980)
Verslag over Het Jaar 1979	1979, end	SEP (1980)
Elektriciteit in Nederland 1980	1980, end	Directie Arnhemse instellingen van de elektriciteitsbedrijven in Nederland (AIe, 1981)
Verslag over Het Jaar 1980	1980, end	SEP (1981)
Elektriciteit in Nederland 1981	1981, end	AIe (1982)
Verslag over Het Jaar 1981	1981, end	SEP (1982)
Verslag over Het Jaar 1982	1982, end	SEP (1983)
Elektriciteit in Nederland 1982	1982, end	AIe (1983)
Elektriciteit in Nederland 1983	1983, end	AIe (1984)
Verslag over Het Jaar 1983	1983, end	SEP (1984)
Elektriciteit in Nederland 1984	1984, end	Directies Arnhemse instellingen van de elektriciteitsbedrijven in Nederland (AIe, 1985)
Elektriciteit in Nederland 1985	1985, end	N.V. Samenwerkende Elektriciteits-Produktiebedrijven et al. (SEP/GKN/KEMA/VEEN/VDEN, 1986)
Verslag over Het Jaar 1984	1985-01-01	SEP (1985)
Elektriciteit in Nederland 1986	1986, end	SEP/GKN/KEMA/VEEN/VDEN (1987)
Verslag over Het Jaar 1985	1986-01-01	SEP (1986)
Verslag over Het Jaar 1986	1986-01-01	SEP (1987)
Elektriciteit in Nederland 1987	1987, end	SEP/GKN/KEMA/VEEN/VDEN (1988)
Verslag over Het Jaar 1987	1987-12-31	SEP (1988)
Elektriciteit in Nederland 1988	1988, end	N.V. Samenwerkende Elektriciteits-Produktiebedrijven et al. (SEP/VEEN/KEMA, 1989)
Verslag over Het Jaar 1988	1988-12-31	SEP (1989)
Elektriciteit in Nederland 1989	1989, end	N.V. Samenwerkende Elektriciteits-Produktiebedrijven and Vereniging van Exploitanten van Elektriciteitsbedrijven in Nederland (SEP/VEEN, 1990)
Verslag over Het Jaar 1989	1989-12-31	SEP (1990)
Elektriciteit in Nederland 1990	1990, end	SEP/VEEN (1991)

Elektriciteit in Nederland 1991	1991, end	SEP/VEEN (1992)
Elektriciteit in Nederland 1992	1992, end	SEP/EnergieNed (1993)
Verslag over Het Jaar 1992	1992-12-31	SEP (1993)
Elektriciteit in Nederland 1993	1993, end	SEP/EnergieNed (1994)
Verslag over Het Jaar 1993	1993-12-31	SEP (1994)
Elektriciteit in Nederland 1994	1994, end	SEP/EnergieNed (1995)
Verslag over Het Jaar 1994	1994-12-31	SEP (1995)
Elektriciteit in Nederland 1995	1995, end	SEP/EnergieNed (1996)
Verslag over Het Jaar 1995	1995-12-31	SEP (1996)
Verslag over Het Jaar 1996	1996-12-31	SEP (1997)
Verslag over Het Jaar 1997	1997-12-31	SEP (1998)
Jaarverslag 2000	2001-01-01	TenneT (2001)
Jaarverslag 2001	2002-01-01	TenneT (2002b)
Nederlands Hoogspanningsnet	2002-01-01	TenneT (2002a)
Jaarverslag 2002	2003-01-01	TenneT (2003)
Nederlands Hoogspanningsnet	2004-01-01	TenneT (2004a)
Jaarverslag 2003	2004-01-01	TenneT (2004b)
Jaarverslag 2004	2005-01-01	TenneT (2005)
Jaarverslag 2005	2006-01-01	TenneT (2006)
Nederlands Transportnet	2007-01-02	TenneT (2007b)
Jaarverslag 2006	2007-04	TenneT (2007a)
Elektriciteitstransportnet TenneT TSO B.V.	2008-04	TenneT (2008)
Jaarverslag 2008	2009-03	TenneT (2009)
Jaarverslag 2009	2010 (?)	TenneT (2010)
Jaarverslag 2010	2011 (?)	TenneT (2011a)
Nederlands Transportnet	2011-01	TenneT (2011b)
Jaarverslag 2011	2012-01-01	TenneT (2012)
Integrated Annual Report TenneT 2012	2012-12-31	TenneT (2013)
Integrated Annual Report TenneT 2013	2014-02-01	TenneT (2014)
Integrated Annual Report 2014 TenneT Holding B.V.	2014-12-31	TenneT (2015)
Integrated Annual Report 2015 TenneT Holding B.V.	2015-12-31	TenneT (2016a)
Netkaart TenneT (Nederland En Duitsland)	2015-12-31	TenneT (2016b)
Nederlands Transportnet 2017	2017, spring	TenneT (2017b)
Netkaart Nederland	2017, spring	TenneT (2017a)
Netkaart (Technical Overview)	2018-07	TenneT (2018)
Netkaart Nederland	2018-12-31	TenneT (2019)
Nederlands Transportnet 2020	2019, autumn	TenneT (2020a)
Netkaart Nederland	2019-12-31	TenneT (2020b)
Netkaart Nederland	2020 (?)	TenneT (2020c)
Netkaart Nederland Offshore	2020 (?)	TenneT (2020d)
Netkaart TenneT	2020 (?)	TenneT (2020e)
Netkaart TenneT	2021-04	TenneT (2021)
Netkaart Offshore Nederland	2021-12-01	TenneT (2022a)
Netkaart Onshore Nederland	2021-12-01	TenneT (2022b)

Appendix C

Existing power grid models

To get an idea of the existing network models of power grids, we inventorized the datasets used in the literature. The results are reported in Table C.1. There are only two datasets that cover a longer time period: the French network from Buzna et al. (2009) and the Hungarian network from Hartmann and Sugár (2021). This shows that a new dataset of the Dutch network would be a valuable addition.

Table C.1: Inventorization of existing network models.

Name	Time period	Nodes	Edges	Voltages (kV)	Reference
France	1960–2000	8–208	6–291	400	Buzna et al. (2009)
WECC network models		1553, 9402, 19 402	2114, 3345, 22 113		Carreras et al. (2012), Carreras et al. (2019)
U.S. Eastern interconnect (NERC)	2003	235 907			Chassin and Posse (2005)
U.S. Western System (WECC)		78 216			Chassin and Posse (2005)
Power Systems Test Case Archive	1962–1993	14–300	20–411	1–345	Christie (1999)
Italy - GRTN		314	517	220, 380	Crucitti et al. (2004)
Anhui province, China	2004	84	112		Han and Ding (2011)
East China	2004	769	1029		Han and Ding (2011)
Hungarian network	1949–2019	10–385	9–504	120, 220, 400, 750	Hartmann and Sugár (2021)
Nordic power grid		4789	5571		Holmgren (2006)
Continental European Transmission Network	2009	1494	2322	110, 138, 220, 380	Hutcheon and Bialek (2013)
Central Chilean power grid	2015–2016	218–347	409–527	<66, 66, 110, 154, 220, 550	Kim et al. (2018)
ELMOD (EU)	2005–2006	2120	3150	110, 220, 380	Leuthold et al. (2012)
SciGRID	2015	1467	2280	220–500	Matke et al. (2016)
Northern European power grid	2009	236	320	220, 275, 400	Menck et al. (2014)
Northern Netherlands (medium voltage)		4185	4574		Pagani and Aiello (2011)
Europe (UCTE)	2003	>3000	4300	110–400	Rosas-Casals et al. (2007)
France (GF)	2005	146	223	400	Rosato et al. (2007)
Italy (GI)	2002	127	171	380	Rosato et al. (2007)
Italy - fine grained (GI2)	2002	1926	2240	120–380	Rosato et al. (2007)
Spain (GS)		98	175	400	Rosato et al. (2007)
British power grid		120	165	300–400	Simonsen et al. (2008)
MATPOWER – Poland (case2746wop, updated)	2003-2004	2746	3340	110, 220, 400	Snodgrass et al. (2022)
NYISO (New York state)		2935	6567		Wang et al. (2010)
Western US Power Grid		4941	6594	345–1500	Watts and Strogatz (1998)
GridKit – Europe	2016	13 871	18 805	10–750	Wiegmans (2016a)
GridKit – North America	2016	22 459	16 174	12–1333	Wiegmans (2016a)
GridKit – ENTSOE-E map extract	2016	7893	9784	132, 220, 300, 380, 500, 750	Wiegmans (2016b)
MATPOWER – Poland (case2383wp)	1999-2000	2383	2886	110, 220, 400	Zimmerman et al. (2011)